

192. Metal-Ion-Coordinating Properties of Various Phosphonate Derivatives, Including 9-[2-(Phosphonylmethoxy)ethyl]adenine (PMEA) – an Adenosine Monophosphate (AMP) Analogue¹⁾ with Antiviral Properties

by Helmut Sigel^{a)}*, Dong Chen^{a)}, Nicolas A. Corfű^{a)}, Fridrich Gregář^{b)}, Antonin Holý^{c)}, and Milan Strašák^{†b)}

^{a)} Institute of Inorganic Chemistry, University of Basel, Spitalstrasse 51, CH-4056 Basel, Switzerland

^{b)} Faculty of Pharmacy, Comenius University, 83232 Bratislava, Czecho-Slovakia

^{c)} Institute of Organic Chemistry and Biochemistry, Czechoslovak Academy of Science, 16610 Prague, Czecho-Slovakia

(17.VIII.92)

The stability constants of the 1:1 complexes formed between Mg^{2+} , Ca^{2+} , Sr^{2+} , Ba^{2+} , Mn^{2+} , Co^{2+} , Ni^{2+} , Cu^{2+} , (in part) Zn^{2+} , or Cd^{2+} and (phosphonylmethoxy)ethane (PME^{2-}) or 9-[2-(phosphonylmethoxy)ethyl]adenine ($PMEA^{2-}$) were determined by potentiometric pH titration in aqueous solution ($I = 0.1M$, $NaNO_3$; 25°). The experimental conditions were carefully selected such that self-association of the adenine derivative $PMEA$ and of its complexes was negligibly small; *i.e.*, it was made certain that the properties of the monomeric $[M(PMEA)]$ complexes were studied. Recent measurements with simple phosphate monoesters, $R-MP^{2-}$ (where R is a non-coordinating residue; S.S. Massoud, H. Sigel, *Inorg. Chem.* **1988**, *27*, 1447), were used to show that analogously simple phosphonates ($R-PO_3^{2-}$) – we studied now the complexes of methyl phosphonate and ethyl phosphonate – fit on the same $\log K_{M(R-MP)}^M / \log K_{M(R-PO_3)}^M$ vs. $pK_{H(R-MP)}^H / pK_{H(R-PO_3)}^H$ straight-line plots. With these reference lines, it could be demonstrated that for *all* the $[M(PME)]$ complexes with the mentioned metal ions an increased complex stability is measured; *i.e.*, a stability higher than that expected for a sole phosphonate coordination of the metal ion. This increased stability is attributed to the formation of five-membered chelates involving the ether oxygen present in the $-O-CH_2-PO_3^{2-}$ residue of PME^{2-} (and $PMEA^{2-}$); the formation degree of the five-membered $[M(PME)]$ chelates varies between *ca.* 15 and 40% for the alkaline earth ions and *ca.* 35 to 65% for 3d ions and Zn^{2+} or Cd^{2+} . Interestingly, for the $[M(PMEA)]$ complexes within the error limits exactly the same observations are made indicating that the same five-membered chelates are formed, and that the adenine residue has no influence on the stability of these complexes, with the exception of those with Ni^{2+} and Cu^{2+} . For these two metal ions, an *additional* stability increase is observed which has to be attributed to a metal ion-adenine interaction giving thus rise to equilibria between three different $[M(PMEA)]$ isomers. These equilibria are analyzed, and for $[Cu(PMEA)]$ it is calculated that 17(\pm 3)% exist as an isomer with a sole Cu^{2+} -phosphonate coordination, 34(\pm 10)% form the mentioned five-membered chelate involving the ether oxygen, and the remaining 49(\pm 10)% are due to an isomer containing also a Cu^{2+} -adenine interaction. Based on various arguments, it is suggested that this latter isomer contains two chelate rings which result from a metal-ion coordination to the phosphonate group, the ether oxygen, and to N(3) of the adenine residue. For $[Ni(PMEA)]$, the isomer with a Ni^{2+} -adenine interaction is formed to only 22(\pm 13)%; for $[Cd(PMEA)]$ and the other $[M(PMEA)]$ complexes if at all, only traces of such an isomer are occurring. In addition, the $[M(PMEA)]$ complexes may be protonated leading to $[M(H \cdot PME)]^+$ species in which the proton is mainly at the phosphonate group, while the metal ion is bound in an adenosine-type fashion to the nucleic base residue. Finally, the properties of $[M(PMEA)]$ and $[M(AMP)]$ complexes are compared, and in this connection it should be emphasized that the ether oxygen which influences so much the stability and structure of the $[M(PMEA)]$ complexes in solution is also crucial for the antiviral properties of $PMEA$.

¹⁾ Abbreviations used: Ado = adenosine; AMP^{2-} and ATP^{4-} = adenosine 5'-mono- and -triphosphate, BuP^{2-} = *n*-butyl phosphate; EtP^{2-} = ethyl phosphonate; $HPMPA^{2-}$ = dianion of (*S*)-9-[3-hydroxy-2-(phosphonylmethoxy)propyl]adenine; L = general ligand; M^{2+} = divalent metal ion; MeP^{2-} = methyl phosphonate; $NPhP^{2-}$ = 4-nitrophenyl phosphate; PhP^{2-} = phenyl phosphate; PME^{2-} = dianion of (phosphonylmethoxy)ethane; $PMEA^{2-}$ = dianion of 9-[2-(phosphonylmethoxy)ethyl]adenine; $RibMP^{2-}$ = *D*-ribose 5'-monophosphate; $R-MP^{2-}$ = phosphate monoester (R may be any organic residue, *e.g.*, phenyl or nucleosidyl); $R-PO_3^{2-}$ = general phosphonate ligand; $TM P^{2-}$ = thymidine 5'-monophosphate; $TuMP^{2-}$ = tubercidin 5'-monophosphate (= 7-deaza- AMP^{2-}); UMP^{2-} = uridine 5'-monophosphate.

Introduction. – About one sixth of all known enzyme systems require adenine-containing cofactors [1], many of these being nucleotides. As the biological activity of most nucleotide systems depends on the presence of metal ions [2], many efforts, especially regarding adenine nucleotides [3–5], have been made to resolve the structure of metal-ion-nucleotide complexes in solution [6–8] and in the solid state [9]. Indeed, the properties of various $[M(AMP)]$ [5] [10^b] and $[M(ATP)]^{2-}$ complexes [3] [8] [11] and the forces which determine their structures in solution are now relatively well understood.

Considering that nucleotides play a key role in many metabolic processes, it is not surprising that artificial nucleotide analogues often display biological activity and that some of them are employed as drugs [12]. One of these active compounds, 9-[2-(phosphonylethyl)adenine] ($PMEA^{2-}$), can be considered as an analogue of adenosine 5'-monophosphate (AMP^{2-} ; see Fig. 1) [6] [8] [13]. Indeed, $PMEA$ and some related

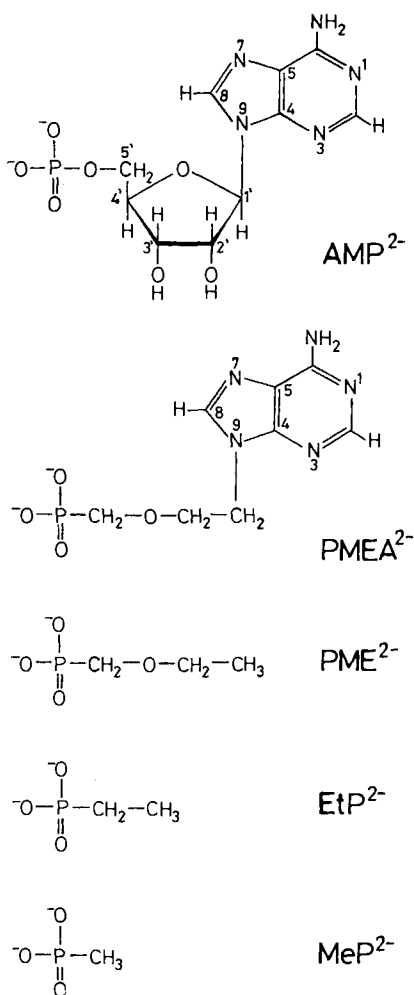
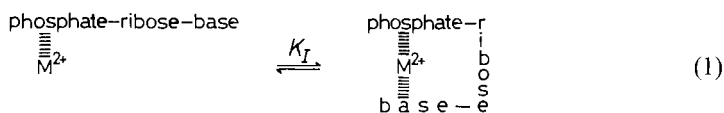


Fig. 1. Chemical structure of the dianion of 9-[2-(phosphonylethyl)adenine] ($PMEA^{2-}$) in comparison with the structures of adenosine 5'-monophosphate (AMP^{2-}), which is shown in its dominating anti-conformation [6] [8] [13], and the dianion of (phosphonylethyl)ethane (PME^{2-}). The other two phosphonate derivatives, i.e. MeP^{2-} and EtP^{2-} , are also employed in this study.

compounds show antiviral properties against DNA viruses, like herpes viruses, adenoviruses, or poxviruses [14–16], and also against retroviruses, *i.e.* human immunodeficiency (HIV) and *Moloney* murine sarcoma viruses (MSV) [14] [16] [17]; moreover, they exhibit a cytostatic effect on L-1210 mouse leukemia cells [14].

PMEA and related phosphonate derivatives are converted by cellular nucleotide kinases into their diphosphates, and as such they inhibit viral and, to a lesser extent, cellular DNA synthesis [14]. In this connection, one may point out that base- or sugar-modified nucleotide analogues with monophosphate-ester residues are known to undergo enzyme-catalyzed dephosphorylation during their passage through the cellular membrane or in blood plasma [18], rendering therapeutic application of such antimetabolites inefficient. This difficulty is circumvented by applying analogues with a phosphonate residue [18].

The potential therapeutic applications of PMEAs and the fact that nucleotide-dependent enzymic systems generally depend on the presence of metal ions prompted us to study the metal-ion-binding properties of PMEA^{2-} . To evaluate the measured stability constants of the $[\text{M}(\text{PMEA})]$ complexes regarding the structure of these complexes in solution, it was also necessary to include (phosphonyl-methoxy)ethane (PME^{2-}) as ligand (see *Fig. 1*). It is important to recall at this point that in various $[\text{M}(\text{AMP})]$ complexes macrochelates are formed giving rise to the intramolecular *Equilibrium 1* where a metal ion binds not only to the phosphate group but also to N(7) of the purine residue [5].



Consequently, the question arises about a similar nucleic base-back binding in certain $[\text{M}(\text{PMEA})]$ complexes. If so: is it possible to quantify the extent of such metal ion-base interactions? Finally, methyl phosphonate (MeP^{2-}) and ethyl phosphonate (EtP^{2-}) (*Fig. 1*) are used in this study as ligands representative for the formation of pure phosphonate-metal ion complexes.

Experimental. – *Materials.* 9-[2-(Phosphonyl-methoxy)ethyl]adenine, *i.e.* the free $\text{H}_2(\text{PMEA})^{\pm}$ acid, was prepared in the laboratory of *A.H.* according to published procedures [19]. (Phosphonyl-methoxy)ethane, *i.e.* $\text{H}_2(\text{PME})$, was synthesized by *F.G.* and coworkers [20]. Methylphosphonic acid, $\text{CH}_3\text{P}(\text{O})(\text{OH})_2$ (*purum*: 98%), was purchased from *Fluka Chemie AG*, Buchs, Switzerland, and ethylphosphonic acid, $\text{CH}_3\text{CH}_2\text{P}(\text{O})(\text{OH})_2$ (98%), from *Aldrich-Chemie GmbH & Co. KG*, Steinheim, FRG. The aq. stock solns. of the phosphonates, R-PO_3^{2-} , were freshly prepared daily by adding 2 equiv. of NaOH; the exact concentration was each time newly determined (see below).

The disodium salt of 1,2-diaminoethane-*N,N,N',N'*-tetraacetic acid ($\text{Na}_2\text{H}_2\text{EDTA}$), potassium hydrogen phthalate, HNO_3 , NaOH (*Titrisol*), and the nitrate salts of Na^+ , Mg^{2+} , Ca^{2+} , Sr^{2+} , Ba^{2+} , Mn^{2+} , Co^{2+} , Ni^{2+} , Cu^{2+} , Zn^{2+} , and Cd^{2+} (all *pro analysi*) were from *Merck AG*, Darmstadt, FRG. All solns. were prepared with distilled CO_2 -free water.

The titer of the NaOH used for the titrations was established with potassium hydrogen phthalate. The exact concentrations of the R-PO_3^{2-} stock solns. used in the experiments with metal ions (titrated in the presence of an excess of HNO_3 ; see below) were measured with NaOH, and the concentrations of the stock solns. of the divalent metal ions were determined *via* their EDTA complexes.

Potentiometric pH Titrations. The pH titrations were carried out with a *Metrohm* E536 potentiograph equipped with a *E655* dosimat and *6.0202.100 (JC)* combined macro glass electrodes. The buffer solns. (pH 4.64, 7.00, 9.00) for calibration were also from *Metrohm*. The direct pH-meter readings were used to calculate the acidity constants; *i.e.*, these constants are so-called practical, mixed or *Bronsted* constants [21]. Their negative logarithms

given for aqueous solutions at $I = 0.1\text{M}$ (NaNO_3) and 25° may be converted into the corresponding concentration constants by subtracting 0.02 log unit [21].

It should be emphasized that the ionic product of water (K_w) and the mentioned conversion term do *not* enter into our calculation procedures, because we evaluate the *differences* in NaOH consumption between the corresponding solns.; *i.e.*, always solns. with and without ligand are titrated (see also below; for further details see [21] [22]).

Determination of Equilibrium Constants. The acidity constants $K_{\text{H(R-PO}_3\text{)}}^{\text{H}}$ for $\text{H}(\text{MeP})^-$, $\text{H}(\text{EtP})^-$ and $\text{H}(\text{PME})^-$ were determined by titrating 50 ml of aq. 0.54 mM HNO_3 and NaNO_3 ($I = 0.1\text{M}$; 25°) in the presence and absence of 0.3 mM R-PO_3^{2-} under N_2 with 1 ml of 0.03M NaOH and by using the differences in NaOH consumption between two such titrations for the calculations. For the determination of $K_{\text{H}_2(\text{PMEA})}^{\text{H}}$ and $K_{\text{H}(\text{PMEA})}^{\text{H}}$ of $\text{H}_2(\text{PMEA})^\pm$, where one proton is at the base moiety and the other at the phosphonate group, the concentration of HNO_3 was increased to 0.85 mM and 2 ml of 0.03M NaOH were used in the titrations. These constants were calculated with a *Hewlett-Packard Vectra 60PC* desk computer (connected with a *Brother M1509* printer and a *Hewlett-Packard 7475A* plotter) by a curve-fit procedure using a *Newton-Gauss* nonlinear-least-squares program within the pH range determined by the lowest point of neutralization reached by the experimental conditions (*ca.* 20% for the equilibrium $\text{H}_2(\text{PMEA})^\pm/\text{H}(\text{PMEA})^-$) and *ca.* 97% neutralization (for the equilibrium $\text{H}(\text{PMEA})^-/\text{PMEA}^{2-}$). In those cases where only the constant $K_{\text{H(R-PO}_3\text{)}}^{\text{H}}$ is applicable, the calculations were carried out between 3% and 97% neutralization. For the acidity constants of $\text{H}(\text{MeP})^-$, $\text{H}(\text{EtP})^-$, $\text{H}(\text{PME})^-$ and $\text{H}_2(\text{PMEA})^\pm$, 24 , 24 , 28 and 20 pairs of independent titrations were made, respectively, and the results averaged.

The stability constants $K_{\text{M(H-PMEA)}}^{\text{M}}$, $K_{\text{M(PMEA)}}^{\text{M}}$, and $K_{\text{M(R-PO}_3\text{)}}^{\text{M}}$, where $\text{R-PO}_3^{2-} = \text{MeP}^{2-}$, EtP^{2-} , or PME^{2-} , were determined under the same conditions as the acidity constants, but NaNO_3 was partly or fully replaced by $\text{M}(\text{NO}_3)_2$. ($I = 0.1\text{M}$, 25°). The ligand/ M^{2+} ratios were $1:111$ (Mg^{2+} , Ca^{2+} , Sr^{2+} , Ba^{2+}), $1:89$ (Mg^{2+} , Ca^{2+} , Sr^{2+} , Ba^{2+}), $1:56$ (Mn^{2+} , Co^{2+} , Zn^{2+} , Cd^{2+}), $1:44$ (Co^{2+} , Ni^{2+}), $1:28$ (Mn^{2+} , Ni^{2+} , Zn^{2+} , Cd^{2+}), and $1:11$ and $1:5.6$ (Cu^{2+}). $K_{\text{M(R-PO}_3\text{)}}^{\text{M}}$ was computed for each pair of titrations by taking into account the species H^+ , $\text{H}(\text{R-PO}_3)^-$, R-PO_3^{2-} , M^{2+} , and $\text{M}(\text{R-PO}_3)$. The data were collected every 0.1 pH unit from *ca.* 5% complex formation to a neutralization degree of *ca.* 85% or to the beginning of the hydrolysis of $\text{M}(\text{aq})^{2+}$, which was evident from the titrations without R-PO_3^{2-} . The values calculated individually for $\log K_{\text{M(R-PO}_3\text{)}}^{\text{M}}$ showed no dependence on pH or on the excess amount of M^{2+} .

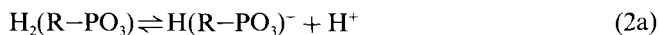
With PMEA , the formation of monoprotonated $[\text{M}(\text{H}\cdot\text{PMEA})]^+$ complexes is of importance. Therefore, $K_{\text{M(H-PMEA)}}^{\text{M}}$ and $K_{\text{M(PMEA)}}^{\text{M}}$ of the $\text{M}^{2+}/\text{PMEA}$ systems were computed for each pair of titrations with a curve-fitting procedure by taking into account the species H^+ , $\text{H}_2(\text{PMEA})^\pm$, $\text{H}(\text{PMEA})^-$, PMEA^{2-} , M^{2+} , $[\text{M}(\text{H}\cdot\text{PMEA})]^+$, and $[\text{M}(\text{PMEA})]$. The experimental data were evaluated up to the point where hydrolysis of $\text{M}(\text{aq})^{2+}$ begins.

All stability constants result from at least six, usually eight independent pairs of titration curves. No stability constants could be determined for the $\text{Zn}^{2+}/\text{PMEA}$ system, as a precipitate formed already at a relatively low pH.

Results and Discussion. – Purines are well known to undergo self-association due to stacking of their nucleic-base-ring systems [23]. In a first approximation, one may assume that the selfstacking tendency of the isocharged species AMP^{2-} and PMEA^{2-} (see *Fig. 1*) is about the same (AMP^{2-} : $K = 2.1 \pm 0.3 \text{ M}^{-1}$, according to the isodesmic model for an indefinite noncooperative self-association). In any case, the self-association of the two-fold negatively charged PMEA^{2-} species will certainly be lower than that of neutral adenosine ($K = 15 \pm 3 \text{ M}^{-1}$) [13] [23] [24], *ca.* 97% of which exist in 1 mM solution in the monomeric form. This is important, because the conditions for the measurements with PMEA had to be selected such that the results refer to monomeric species, *i.e.* that no self-association occurs. With $[\text{PMEA}] = 3 \cdot 10^{-4} \text{ M}$ (see *Experimental*) and by considering the mentioned equilibrium constants for self-association this condition is certainly achieved. Of course, the other phosphonate derivatives considered in this study do not undergo self-association due to the lack of an aromatic moiety; however, for the sake of uniformity in these cases also the mentioned low concentrations (0.3 mM) were employed.

1. *Some Considerations on the Acidity Constants of Diprotonated Phosphonate Groups in $\text{H}_2(\text{R-PO}_3)$ Species and in $\text{H}_3(\text{PMEA})^+$.* Simple phosphonate species (R-PO_3^{2-}), such as methyl phosphonate ($\text{CH}_3\text{PO}_3^{2-}$, MeP^{2-}), are dibasic species that may carry two protons

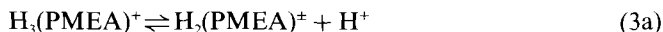
at their phosphonate group. The first proton is released at a rather low pH, and its acidity constant (*Eqn. 2*)



$$K_{\text{H}_2(\text{R}-\text{PO}_3)}^{\text{H}} = [\text{H}(\text{R}-\text{PO}_3)^-][\text{H}^+]/[\text{H}_2(\text{R}-\text{PO}_3)] \quad (2b)$$

was, therefore, not measured, but estimated based on the following reasoning: comparison of the $\text{p}K_{\text{a}}$ values for $\text{CH}_3\text{O}-\text{P}(\text{O})_2(\text{OH})^-$ and $\text{CH}_3-\text{P}(\text{O})_2(\text{OH})^-$ indicates that replacement of an O–P bond by a C–P bond increases the basicity by *ca.* 1.3 log units (*Table 1*; *vide infra*). As previously a $\text{p}K_{\text{a}}$ of 0.7 ± 0.3 ($I = 0.1\text{M}$, NaNO_3 ; 25°) was estimated for the release of a proton from a R–O–P(O)(OH)₂ group, *i.e.* for $\text{H}_2(\text{UMP})$ [25], we may estimate $\text{p}K_{\text{H}_2(\text{R}-\text{PO}_3)}^{\text{H}} \approx 2.0$ (*Eqn. 2*) for a R–P(O)(OH)₂ group. Indeed this value is in perfect agreement with $\text{p}K_{\text{a}} = 2.0$ for the release of the first proton from phosphonic acid, $\text{HP}(\text{O})(\text{OH})_2$ [26].

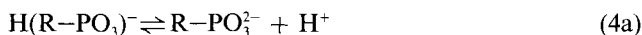
Similarly, the release of the first proton of the phosphate group from the positively charged $\text{H}_3(\text{AMP})^+$ occurs with $\text{p}K_{\text{a}} = 0.4 \pm 0.2$ ($I = 0.1\text{M}$, NaNO_3 ; 27°) [13]; hence, one may estimate for the release of the first proton from the phosphonate group in $\text{H}_3(\text{PMEA})^+$, $\text{p}K_{\text{H}_3(\text{PMEA})}^{\text{H}} \approx 1.7$ (*Eqn. 3*).



$$K_{\text{H}_3(\text{PMEA})}^{\text{H}} = [\text{H}_2(\text{PMEA})^+][\text{H}^+]/[\text{H}_3(\text{PMEA})^+] \quad (3b)$$

Overall we may conclude that the release of the first proton from the phosphonate group in all the phosphonate ligands considered (*Fig. 1*) occurs (to be on the safe side) with $\text{p}K_{\text{a}} < 2.5$. This demonstrates that none of the other deprotonation equilibria considered below in *Sect. 2*, nor any of the complex formations (see *Sect. 3*, 5, and 8) is affected by the release of this first proton from a diprotonated phosphonate group.

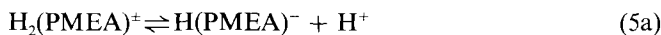
2. *Measured Acidity Constants of Several Monoprotonated Phosphonate Derivatives, $\text{H}(\text{R}-\text{PO}_3)^-$, and of $\text{H}_2(\text{PMEA})^\pm$.* The equilibrium for the release of the second proton from the phosphonate group of methyl phosphonate, ethyl phosphonate, and (phosphorylmethoxy)ethane (*Fig. 1*) is expressed in *Eqn. 4*:



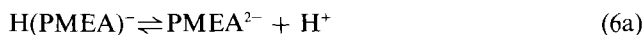
$$K_{\text{H}(\text{R}-\text{PO}_3)}^{\text{H}} = [\text{R}-\text{PO}_3^{2-}][\text{H}^+]/[\text{H}(\text{R}-\text{PO}_3)^-] \quad (4b)$$

The corresponding results of the potentiometric pH titrations are listed in *Table 1* together with some related data taken from the literature [5] [13] [27].

In the zwitterionic species $\text{H}_2(\text{PMEA})^\pm$ (see also *Eqn. 3* in *Sect. 1*), the first proton is released from the base residue (*Eqn. 5*), while the final proton, now from $\text{H}(\text{PMEA})^-$, is again from the phosphonate group (*Eqn. 6*):



$$K_{\text{H}_2(\text{PMEA})}^{\text{H}} = [\text{H}(\text{PMEA})^-][\text{H}^+]/[\text{H}_2(\text{PMEA})^\pm] \quad (5b)$$



$$K_{\text{H}(\text{PMEA})}^{\text{H}} = [\text{PMEA}^{2-}][\text{H}^+]/[\text{H}(\text{PMEA})^-] \quad (6b)$$

Evidently *Equilibria 4* and *6* correspond to each other, in both cases the final proton is released from the phosphonate group in a single-charged species.

Table 1. *Negative Logarithms of the Acidity Constants of the Protonated Phosphonate Ligands Considered in this Study (see Fig. 1), as well as for Some Related Species, as Determined by Potentiometric pH Titrations in Aqueous Solution at 25° and I = 0.1 M (NaNO₃)^a*

Acid	pK _a for the sites		Ref.
	≧N(1)H ⁺ (Eqn. 5)	-P(O) ₂ (OH) ⁻ (Eqns. 4, 6)	
CH ₃ OP(O) ₂ (OH) ⁻		6.2 ^b	[27]
CH ₃ P(O) ₂ (OH) ⁻ , H(MeP) ⁻		7.53 ± 0.01	^c)
C ₂ H ₅ P(O) ₂ (OH) ⁻ , H(EtP) ⁻		7.77 ± 0.01	^c)
H(PME) ⁻		7.02 ± 0.01	^c)
H ₂ (PMEA) [±]	4.16 ± 0.02	6.90 ± 0.01	^c)
H ₂ (AMP) [±]	3.84 ± 0.02	6.21 ± 0.01	[5]
H(adenosine) ⁺	3.61 ± 0.03		[13]

^a) So-called practical constants [21] are listed; see *Experimental*. The errors given are *three times* the standard error of the mean value or the sum of the probable systematic errors, whichever is larger.
^b) I = 0.1 M, NaCl; 25° [27].
^c) This work.

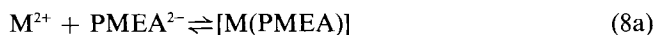
From the results summarized in *Table 1* and the comparison among the values listed for H(adenosine)⁺, H₂(AMP)[±], and H₂(PMEA)[±] follows unequivocally that the first proton released from these species originates from the same site: indeed, N(1) of the adenine residue (for details regarding adenosine and AMP, see [13]) is well known [28] as being the most basic site (see *Fig. 1*).

The increased acidity of CH₃O-P(O)₂(OH)⁻ compared with CH₃-P(O)₂(OH)⁻ (see *Table 1*) is clearly due to the electron-withdrawing properties of the CH₃O group. This effect is still seen if the O-atom is separated by a C-atom from the P-atom, as the comparison of the pK_a values for H(MeP)⁻ and H(EtP)⁻ with H(PME)⁻ and H(PMEA)⁻ (see *Fig. 1*) demonstrates. Smaller differences in the pK_a values, like those between H(PME)⁻ and H(PMEA)⁻, are probably mainly connected with different solvation properties of the dianionic species [25] [29].

3. *Stabilities of the Complexes Formed between PMEAs Species and Divalent Metal Ions.* The experimental data of the potentiometric pH titrations of the M²⁺/PMEA systems are completely described by *Equilibria 5–8*,

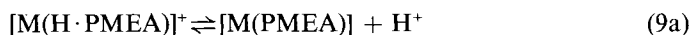


$$K_{[M(H \cdot PME A)]}^M = \frac{[M(H \cdot PME A)]^{+}}{[M^{2+}][H(PMEA)^{-}]} \quad (7b)$$



$$K_{[M(PMEA)]}^M = \frac{[M(PMEA)]}{[M^{2+}][PME A^{2-}]} \quad (8b)$$

if the evaluation is not carried into the pH range, where formation of hydroxo complexes occurs. The acidity constant of the connected *Equilibrium 9* may be calculated with *Eqn. 10*.



$$K_{[M(H \cdot PME A)]}^H = \frac{[M(PMEA)][H^{+}]}{[M(H \cdot PME A)]^{+}} \quad (9b)$$

$$pK_{[M(H \cdot PME A)]}^H = pK_{H(PMEA)}^H + \log K_{[M(H \cdot PME A)]}^M - \log K_{[M(PMEA)]}^M \quad (10)$$

Table 2. Logarithms of the Stability Constants of $[M(H \cdot PME A)]^+$ (Eqn. 7) and $[M(PME A)]$ Complexes (Eqn. 8) as Determined by Potentiometric pH Titrations in Aqueous Solution, Together with the Negative Logarithms of the Acidity Constants (Eqns. 9 and 10) of the Corresponding $[M(H \cdot PME A)]^+$ Complexes at 25° and I = 0.1M ($NaNO_3$)^{a)}b)

M^{2+}	$\log K_{[M(H \cdot PME A)]}^M$	$\log K_{[M(PME A)]}^M$	$pK_{[M(H \cdot PME A)]}^H$ ^{d)}
Mg^{2+}	~ 0.0 ^{c)}	1.87 ± 0.04	~ 5.0
Ca^{2+}	~ 0.0 ^{c)}	1.65 ± 0.05	~ 5.3
Sr^{2+}	~ 0.0 ^{c)}	1.37 ± 0.03	~ 5.5
Ba^{2+}	~ 0.0 ^{c)}	1.30 ± 0.05	~ 5.6
Mn^{2+}	0.3 ± 0.5	2.54 ± 0.06	4.7 ± 0.5
Co^{2+}	0.59 ± 0.12	2.37 ± 0.03	5.12 ± 0.12
Ni^{2+}	0.96 ± 0.23	2.41 ± 0.05	5.45 ± 0.24
Cu^{2+}	1.48 ± 0.16	3.96 ± 0.04	4.42 ± 0.17
Cd^{2+}	1.00 ± 0.21	3.00 ± 0.04	4.90 ± 0.21

a) The errors given are *three times* the standard error of the mean value or the sum of the probable systematic errors, whichever is larger. The error limits of the derived data, in the present case for $pK_{[M(H \cdot PME A)]}^H$, were calculated according to the error propagation after Gauss.

b) The $Zn^{2+}/PME A$ system could not be studied due to precipitation (see also *Experimental*). An estimated stability constant for the $[Zn(PME A)]$ complex is given in *Footnote c* of Table 7.

c) These values could not be determined as the formation degree of the $[M(H \cdot PME A)]^+$ species under our experimental conditions was very low; we estimate for all these cases $\log K_{[M(H \cdot PME A)]}^M \approx 0.0 (\pm 0.5)$.

d) These values were calculated according to Eqn. 10 by using the acidity constants of Table 1 and the stability constants listed above.

The constants for *Equilibria 7–9* are listed in Table 2. Clearly, the analysis of potentiometric pH titrations yields only the amount and distribution of species of a net charged type, e.g. of $[M(H \cdot PME A)]^+$, and further information is required to locate the binding sites of the proton and the metal ion (see *Sect. 4*).

Similarly, the stability constants of the $[M(PME A)]$ complexes also warrant a more detailed analysis regarding the structure of these complexes in solution. For example, the acidity constants of $H(PME A)^-$ ($pK_{H(PME A)}^H = 6.90$; Table 1) and $H_2PO_4^-$ ($pK_{H_2PO_4}^H = 6.70$ [30]) differ by only 0.2 log unit, while, e.g. the stability constants of the $[Ni(PME A)]$ and $[Cu(PME A)]$ complexes are by ca. 0.35 and 0.75 log unit, respectively, more stable than the corresponding $[M(HPO_4)]$ complexes [30]. This increased stability indicates that aside from the phosphonate group other binding sites are participating in the $[M(PME A)]$ complexes. This problem will be dealt with in *Sect. 7, 9, and 10*. However, the fact that the stability of the $[M(PME A)]$ complexes does not strictly follow the *Irving-Williams* series [31] shows that it is mainly governed by the metal-ion affinity of the PO_3^{2-} group; this deviation from the *Irving-Williams* series is already a long standing experience for phosphate complexes [25] [30] [32].

4. *Structural Considerations on the Monoprotonated $[M(H \cdot PME A)]^+$ Complexes.*
A comparison of the acidity constants of $H_2(PME A)^{\pm}$, $pK_{H_2(PME A)}^H = 4.16$ and $pK_{H(PME A)}^H = 6.90$ (Table 1), with the acidity constants of the $[M(H \cdot PME A)]^+$ complexes according to *Equilibrium 9*, which are listed in the fourth column of Table 2, demonstrates that the metal ion must be mainly located at the adenine residue and the proton at the phosphonate group in these complexes. That a proton located at a certain site in a ligand must be acidified upon metal-ion binding is evident: from the mentioned data follows that this is observed only, if the proton-binding is attributed to the phosphonate group;

consequently, the metal ion has to be located at the adenine residue. This agrees also with the course of the stability constants which follow the *Irving-Williams* series [31] and are typical for binding of metal ions to N sites [32] (*cf.* also the course of the constants listed in columns 2 and 3 of *Table 2*). Of course, isomeric equilibria could also be envisaged [33], though hardly in the present cases.

For some of the metal ions listed in *Table 2* the stability constants of the corresponding $[M(\text{adenosine})]^{2+}$ complexes are also known [28] and given in the second column of *Table 3*. For a direct comparison of these data with those of column 2 of *Table 2* it is necessary to take the slightly different basicities of the N(1) site in H(PMEA)^- and adenosine into account: i.e., $\Delta \text{p}K_a = \text{p}K_{\text{H}_2(\text{PMEA})}^{\text{H}} - \text{p}K_{\text{H}(\text{Ado})}^{\text{H}} = 4.16 - 3.61 = 0.55$ (see *Table 1*). By applying the slopes of the correlation lines for $\log K$ vs. $\text{p}K_a$ plots as given earlier [28] for N(1)- and N(7)-type ligands (see column 3 of *Table 3*) and $\Delta \text{p}K_a = 0.55$, one may calculate 'expected' stability constants for metal-ion binding to the adenine residue in H(PMEA)^- . Comparison of these calculated (*calc.*) constants given in column 4 of *Table 3* with the measured (*exper.*) ones in column 5, leads to the differences listed in column 6 of *Table 3*.

Table 3. *Stability-Constant Comparison for Several $[M(\text{Adenosine})]^{2+}$ and $[M(\text{H} \cdot \text{PMEA})]^+$ Complexes*

M^{2+}	$\log K_{[M(\text{Ado})]}^M$ ^{a)}	m ^{b)}	$\log K_{[M(\text{H} \cdot \text{PMEA})]}^M$		$\log \Delta$ ^{c)}
			<i>calc.</i> ^{c)}	<i>exper.</i> ^{d)}	
Mn^{2+}	-0.8 ± 0.5	0.28	-0.65 ± 0.5	0.3 ± 0.5	0.95 ± 0.7
Co^{2+}	-0.03 ± 0.5	0.26	0.11 ± 0.5	0.59 ± 0.12	0.48 ± 0.5
Ni^{2+}	0.32 ± 0.12	0.31	0.49 ± 0.12	0.96 ± 0.23	0.47 ± 0.26
Cu^{2+}	0.80 ± 0.12	0.46	1.05 ± 0.12	1.48 ± 0.16	0.43 ± 0.20
Cd^{2+}	0.11 ± 0.2	0.33	0.29 ± 0.2	1.00 ± 0.21	0.71 ± 0.29

a) These constants are taken from the two final columns in *Table 4* of [28]; they are the averages of the constants determined in various laboratories.

b) Averages of the slopes (m) for $\log K_{M(L)}^M$ vs. $\text{p}K_{\text{HL}}^{\text{H}}$ correlations for imidazole-like and pyridine-like ligands (L) as listed in *Table 1* of [28].

c) These calculated (*calc.*) values refer to complexes formed with an adenine moiety that has $\text{p}K_a = 4.16$; i.e., the difference $0.55 (= \Delta \text{p}K_a = \text{p}K_{\text{H}_2(\text{PMEA})}^{\text{H}} - \text{p}K_{\text{H}(\text{Ado})}^{\text{H}} = 4.16 - 3.61)$ times the slope m was added to the $\log K_{[M(\text{Ado})]}^M$ values of column two. These stability corrections (in average 0.18 log unit), based on the $[M(\text{Ado})]^+$ complexes, reflect the difference in basicity of N(1) between H(PMEA)^- and Ado; of course, this difference certainly has its origin to a large part in the negative charge of the H(PMEA)^- species. However, it should be emphasized that the effect of the negatively charged $\text{P(O)}_2(\text{OH})^-$ residue on the twofold positively charged metal ion bound to the adenine moiety (*e.g.*, to N(7)) has not yet been taken into account [22]; see also text in *Sect. 4*. The error limits given with the above values are the same as in column two.

d) The measured (*exper.*) values are from column two of *Table 2*.

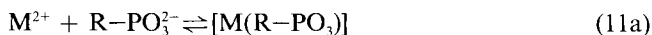
e) $\log \Delta = \log K_{\text{exper.}} - \log K_{\text{calc.}}$ (see the two columns to the left).

At this point, it should be noted that the effect of a single negative charge as present in the $\text{P(O)}_2(\text{OH})^-$ residue on a twofold positively charged metal ion is larger than on the single-charged proton [22]. Clearly, the latter effect has been considered in the calculations for column 4 of *Table 3* (see also *Footnote c* of this *Table*), yet the $(-/2+)$ effect for the metal ions has not yet been taken into account. In previous considerations on a nucleotide-ligand system, with about the same distance between the charged sites, it was concluded [22] that metal-ion binding should be promoted by *ca.* 0.4 log unit due to such an effect. The $\log \Delta$ values given in column 6 of *Table 3* are within their error limits exactly

in this order; this means, the increased stability of the $[M(H \cdot PME A)]^+$ complexes can be explained solely by a charge effect, and there is no need to postulate, *e.g.*, chelate formation between a N(7)-bound metal ion and the $P(O)_2(OH)^-$ residue (though the occurrence of a small percentage of such a chelated species can, of course, not be excluded).

Finally, the present evaluation only proves that in $[M(H \cdot PME A)]^+$ the metal ion is predominantly adenine-bound, but it does not allow a conclusion about the distribution of the metal ions between the N(1) and N(7) sites (*Fig. 1*). However, in a recent study about the dichotomy of metal-ion binding in $[M(Ado)]^{2+}$ complexes, it was concluded [28], that Ni^{2+} and Cu^{2+} , and probably also Co^{2+} and Cd^{2+} , prefer the N(7) site, in contrast to the proton which strongly favors N(1) (which is presumably also preferred by Mn^{2+}).

5. *Stabilities of Complexes with a Pure Phosphonate-Metal-Ion Coordination.* In the last paragraph of *Sect. 3*, it was concluded that the $[M(PME A)]$ complexes are more stable than expected for a sole phosphonate-metal-ion coordination. For a quantitative evaluation of this effect, detailed knowledge on the relation between complex stability ($\log K$) and phosphonate group basicity (pK_a) is necessary. Therefore, we measured the stability constants of various metal-ion complexes formed with methyl phosphonate and ethyl phosphonate by considering *Equilibria 4* and *11* (see columns 2 and 5 of *Table 4*).



$$K_{[M(R-PO_3)]}^M = \frac{[M(R-PO_3)]}{[M^{2+}][R-PO_3^{2-}]} \quad (11b)$$

A C-P bond, compared to an O-P bond, in the residue R should affect only the acidity of the $P(O)_2(OH)^-$ group in $R-PO_3H^-$ species, but it should not have any steric influence on the binding of metal ions to a PO_3^{2-} group. Hence, the previously established

*Table 4. Logarithms of the Stability Constants of $[M(CH_3PO_3)]$ and $[M(CH_3CH_2PO_3)]$ Complexes (Eqn. 11) as Determined by Potentiometric pH Titrations (exper.^a) in Water at 25° and $I = 0.1 M$ ($NaNO_3$). The calculated stability constants for a pure metal-ion-phosphonate coordination (calc.) are given for comparison; these values are based on straight-line equations [5] [25], quantifying the relationship between complex stability and phosphate-group basicity (see also *Fig. 2* and *Sect. 6*)^b and the $pK_{H(R-PO_3)}^H$ values of $H(CH_3PO_3)^-$ and $H(CH_3CH_2PO_3)^-$ (see *Table 1*)*

M^{2+}	$\log K_{[M(CH_3PO_3)]}^M$		$\log A_{MeP}^c$	$\log K_{[M(CH_3CH_2PO_3)]}^M$		$\log A_{EtP}^c$
	exper. ^a	calc. ^b		exper. ^a	calc. ^b	
Mg^{2+}	1.86 ± 0.02	1.86 ± 0.04	0.00 ± 0.04	1.85 ± 0.03	1.91 ± 0.04	-0.06 ± 0.05
Ca^{2+}	1.64 ± 0.03	1.66 ± 0.05	-0.02 ± 0.06	1.61 ± 0.05	1.70 ± 0.05	-0.09 ± 0.07
Sr^{2+}	1.36 ± 0.02	1.36 ± 0.05	0.00 ± 0.05	1.35 ± 0.03	1.38 ± 0.05	-0.03 ± 0.06
Ba^{2+}	1.29 ± 0.02	1.26 ± 0.05	0.03 ± 0.05	1.30 ± 0.03	1.27 ± 0.05	0.03 ± 0.06
Mn^{2+}	2.48 ± 0.02	2.49 ± 0.07	-0.01 ± 0.07	2.51 ± 0.03	2.55 ± 0.07	-0.04 ± 0.08
Co^{2+}	2.24 ± 0.02	2.24 ± 0.07	0.00 ± 0.07	2.27 ± 0.03	2.30 ± 0.07	-0.03 ± 0.08
Ni^{2+}	2.25 ± 0.05	2.32 ± 0.06	-0.07 ± 0.08	2.30 ± 0.05	2.39 ± 0.06	-0.09 ± 0.08
Cu^{2+}	3.49 ± 0.05	3.47 ± 0.08	0.02 ± 0.09	3.61 ± 0.04	3.57 ± 0.08	0.04 ± 0.09
Zn^{2+}	2.60 ± 0.03	2.54 ± 0.08	0.06 ± 0.09	2.67 ± 0.04	2.62 ± 0.08	0.05 ± 0.09
Cd^{2+}	2.90 ± 0.03	2.85 ± 0.06	0.05 ± 0.07	2.94 ± 0.02	2.93 ± 0.06	0.01 ± 0.06

^a) See *Footnote a* of *Table 2*.

^b) The parameters of the straight-line equations are listed in *Table 5* of [25]; the error limits (3σ) are from *Table 6* of [25] (see also *Table 1* in [5]).

^c) $\log A_{R-PO_3} = \log K_{\text{exper.}} - \log K_{\text{calc.}}$; error limits: 3σ .

correlation lines between complex stability and ligand basicity for simple phosphate monoesters ($R-O-PO_3^{2-}$) [25] should also hold for the two mentioned simple phosphonate ligands. Therefore, we used the corresponding acidity constants, $pK_{H(R-PO_3)}^H$, of Table 2 together with the mentioned correlation lines and calculated the expected stability constants for the $[M(MeP)]$ and $[M(EtP)]$ complexes (see columns 3 and 6 of Table 4).

The differences $\log A_{R-PO_3}$ between the experimentally measured (exper.) and the calculated (calc.) stability constants for the $[M(MeP)]$ and $[M(EtP)]$ complexes are zero within the error limits (columns 4 and 7 of Table 4). This means, the data for the complexes of simple phosphate monoesters as well as of phosphonates fit on the same correlation line for a given metal ion. This confirms the expectation expressed above about the lack of a steric influence of a C–P bond compared to an O–P bond in $R-PO_3^{2-}$ species.

6. *Correlation between Complex Stability and Ligand Basicity: Construction of Base Lines for $\log K_{[M(R-PO_3)]}^M$ vs. $pK_{H(R-PO_3)}^H$ Plots.* The result summarized in the last paragraph of the preceding section allows to construct now improved correlation lines including also phosphonates. The straight-line equations on which the calculated stability constants of Table 4 are based had solely been established with phosphate-ester ligands which encompassed only a pK_a range from 5 to 6.7. These data [25] together with the present ones allow now an extension up to a pK_a of 7.8 ($pK_{H(EtP)}^H = 7.77$; Table 1). This means, the acidity constant, $pK_{H(PMEA)}^H = 6.90$, of $H(PMEA)^-$ is then clearly within the covered pK_a range allowing thus valid conclusions about the stability and structure of the $[M(PMEA)]$ complexes (cf. Sect. 7, 9, and 10).

The equilibrium constants for the previously studied phosphate monoester systems, i.e. 4-nitrophenyl phosphate ($NPhP^{2-}$), phenyl phosphate (PhP^{2-}), *n*-butyl phosphate (BuP^{2-}), D-ribose 5'-monophosphate ($RibMP^{2-}$), uridine 5'-monophosphate (UMP^{2-}), and thymidine 5'-monophosphate (TMP^{2-}), furnish six data points. Together with the two phosphonate systems studied now, i.e. $CH_3PO_3^{2-}$ and $CH_3CH_2PO_3^{2-}$ (Sect. 5), in total eight data points are available in the pH range 5–8 for the construction of straight lines from $\log K_{[M(R-MP)]}^M$ or $\log K_{[M(R-PO_3)]}^M$ vs. $pK_{H(R-MP)}^H$ or $pK_{H(R-PO_3)}^H$ plots. The results of the corresponding least-squares calculations are summarized in Table 5. Comparison of these

Table 5. *Base-Line Correlations for M^{2+} -Phosphate or -Phosphonate Complex Stabilities and Phosphate- or Phosphonate-Group Basicities.* Slopes (m) and intercepts (b) for the straight-base-line plots of $\log K_{[M(R-MP)]}^M$ or $\log K_{[M(R-PO_3)]}^M$ vs. $pK_{H(R-MP)}^H$ or $pK_{H(R-PO_3)}^H$ as calculated by the least-squares procedure from the experimental equilibrium constants given in Tables 1, 2, and 4 of [25] for $NPhP^{2-}$, PhP^{2-} , BuP^{2-} , $RibMP^{2-}$, UMP^{2-} and TMP^{2-} , and in Tables 1 and 4 of this work for MeP^{2-} ($CH_3PO_3^{2-}$) and EtP^{2-} ($CH_3CH_2PO_3^{2-}$) ($I = 0.1M$, $NaNO_3$; 25°)^a.

M^{2+}	m	b	R^b	M^{2+}	m	b	R^b
Mg^{2+}	0.208 ± 0.015	0.272 ± 0.097	0.985	Co^{2+}	0.223 ± 0.026	0.554 ± 0.167	0.963
Ca^{2+}	0.131 ± 0.020	0.636 ± 0.131	0.935	Ni^{2+}	0.245 ± 0.023	0.422 ± 0.147	0.975
Sr^{2+}	0.082 ± 0.016	0.732 ± 0.102	0.905	Cu^{2+}	0.465 ± 0.025	-0.015 ± 0.164	0.991
Ba^{2+}	0.087 ± 0.016	0.622 ± 0.107	0.907	Zn^{2+}	0.345 ± 0.026	-0.017 ± 0.171	0.983
Mn^{2+}	0.238 ± 0.022	0.683 ± 0.144	0.975	Cd^{2+}	0.329 ± 0.019	0.399 ± 0.127	0.990

^a) Straight-line equation: $y = mx + b$; where x represents the pK_a value of any phosphate monoester or phosphonate ligand and y the calculated stability constant ($\log K$) of the corresponding $[M(R-MP)]$ or $[M(R-PO_3)]$ complex. The errors given with m and b correspond to one standard deviation (1σ).

^b) Correlation coefficient.

results with the previous calculations given in Table 5 of [25] shows that for all ten systems the error limits for the slopes (m) and intercepts (b) of the least-squares lines overlap within a single standard deviation, confirming again that phosphate monoester and phosphonate systems fit on the same reference lines.

Table 6 lists the deviations from the least-squares line for each individual complex with the eight mentioned phosphate and phosphonate ligands. The points for the TMP systems (column 7 of Table 6) are farthest below the least-squares lines, and those for the PhP systems (column 3) give the most positive deviations; however, *all* deviations are within ± 0.09 log unit. These results also confirm [25] that the RibMP, UMP, and TMP systems have the properties of simple monophosphate esters in aqueous solution (see the deviations listed in columns 5, 6, and 7, respectively, of Table 6). Moreover, the available [25] earlier equilibrium data for HPO_4^{2-} [30] and $\text{CH}_3\text{OPO}_3^{2-}$ [27] [34], the simplest phosphate ligands one may think of, also fit in average within ± 0.06 log unit (for the ten available systems) [25] on the straight lines defined in Table 5 confirming further the validity of the present reference lines.

Table 6. Logarithmic Differences between the Experimental Stability Constants ($\log K_{[M(R-MP)]}^M$ of Tables 2 and 4 in [25], and $\log K_{[M(R-PO_3)]}^M$ of Table 4 in This Study) of the M^{2+} Complexes for NPhP^{2-} , PhP^{2-} , BuP^{2-} , RibMP^{2-} , UMP^{2-} , TMP^{2-} , MeP^{2-} ($\text{CH}_3\text{PO}_3^{2-}$), and EtP^{2-} ($\text{CH}_3\text{CH}_2\text{PO}_3^{2-}$) and the Least-Squares Lines of $\log K_{[M(R-MP)]}^M$ or $\log K_{[M(R-PO_3)]}^M$ vs. $pK_{\text{H}(R-MP)}^{\text{H}}$ or $pK_{\text{H}(R-PO_3)}^{\text{H}}$ Plots (Table 5) as Determined by the Mentioned Eight Complex Systems^{a)}

M^{2+}	[M(NPhP)]	[M(PhP)]	[M(BuP)]	[M(RibMP)]	[M(UMP)]	[M(TMP)]	[M(MeP)]	[M(EtP)]	SD
Mg^{2+}	-0.03	0.04	0.02	0.01	0.01	0.04	0.02	-0.04	0.011
Ca^{2+}	-0.04	0.05	0.04	0.03	0.00	-0.07	0.02	-0.04	0.016
Sr^{2+}	-0.03	0.05	0.02	0.01	0.01	-0.06	0.01	-0.02	0.012
Ba^{2+}	0.00	0.06	0.01	0.01	-0.03	-0.07	0.01	0.00	0.013
Mn^{2+}	-0.01	0.04	0.06	0.03	-0.04	-0.09	0.00	-0.02	0.017
Co^{2+}	-0.03	0.08	0.03	0.05	-0.06	-0.08	0.01	-0.02	0.019
Ni^{2+}	-0.07	0.05	0.01	0.05	0.04	-0.06	-0.02	-0.03	0.017
Cu^{2+}	0.00	0.07	0.01	0.07	-0.07	-0.07	0.00	0.01	0.019
Zn^{2+}	0.00	0.07	0.00	0.07	-0.08	-0.07	0.02	0.01	0.020
Cd^{2+}	-0.01	0.06	0.00	0.04	-0.04	-0.07	0.02	-0.02	0.015

^{a)} The farthest column to the right gives the standard deviation (SD) resulting from the listed differences.

To provide a reliable error limit for any stability constant calculated with the equations of Table 5 and a given pK_a value for each of the ten metal ions studied, the standard deviation of the eight data points from the relevant least-squares line was calculated (Table 6, heading 'SD'). Users of the results described in this section are recommended to apply the equations of Table 5 for phosphate or phosphonate ligands in the pK_a range 5–8 and to consider as error limits for the calculated stability constants, $\log K_{[M(R-MP)]}^M$ or $\log K_{[M(R-PO_3)]}^M$, 2 or 3 times the standard deviation (SD) given in Table 6 for the corresponding metal-ion system. An application of this procedure is given below in Sect. 7 with the evaluation of the [M(PMEA)] stability data of Sect. 3.

7. Proof for an Increased Stability of the [M(PMEA)] Complexes. The tentative conclusion (last paragraph of Sect. 3) about the increased stability of the [M(PMEA)] complexes can now definitely be resolved with the correlations outlined in the preceding Sect. 6:

Plots of $\log K_{[M(R-PO_3)]}^M$ vs. $pK_{H(R-PO_3)}^H$ are shown in Fig. 2 for the 1:1 complexes of Mg^{2+} , Mn^{2+} , and Cu^{2+} with the eight simple ligands mentioned in Sect. 6 allowing only a $R-PO_3^{2-}$ -metal ion binding. The corresponding least-squares base lines define the relation between phosphonate-complex stability and phosphonate-group basicity. The three solid points in Fig. 2 which refer to $[Mg(PMEA)]$, $[Mn(PMEA)]$, and $[Cu(PMEA)]$ are considerably above their reference lines, thus proving an increased stability for these complexes.

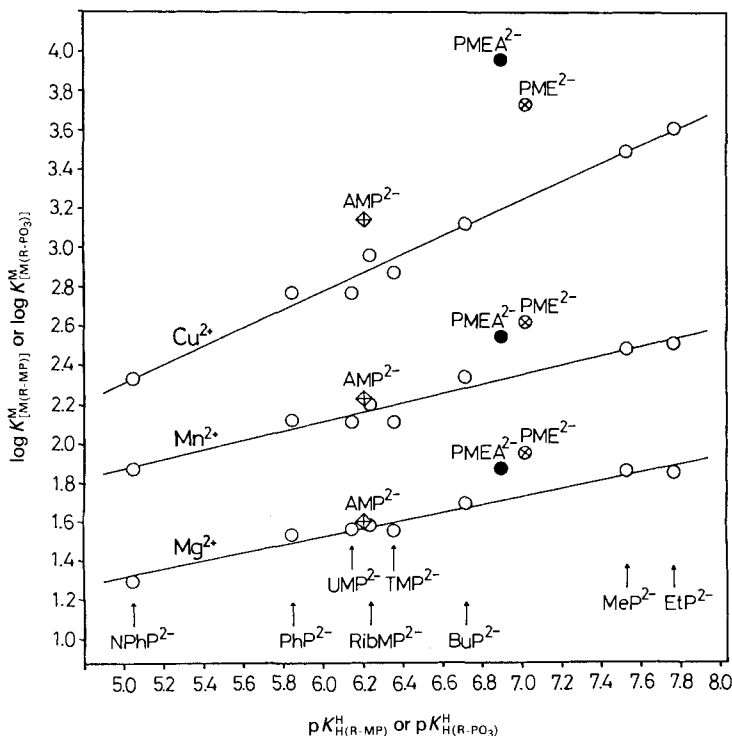


Fig. 2. Evidence for an enhanced stability of several $[M(PMEA)]$ (●), $[M(AMP)]$ (⊕), and $[M(PME)]$ (⊗) complexes, based on the relationship between $\log K_{[M(R-MP)]}^M$ or $\log K_{[M(R-PO_3)]}^M$, and $pK_{H(R-MP)}^H$ or $pK_{H(R-PO_3)}^H$ for the 1:1 complexes of Mg^{2+} , Mn^{2+} , and Cu^{2+} with some simple phosphate monoester ($R-MP^{2-}$) or phosphonate ($R-PO_3^{2-}$) ligands: 4-nitrophenyl phosphate ($NPhP^{2-}$), phenyl phosphate (PhP^{2-}), uridine 5'-monophosphate (UMP^{2-}), D-ribose 5'-monophosphate ($RibMP^{2-}$), thymidine 5'-monophosphate (TMP^{2-}), n-butyl phosphate (BuP^{2-}), methyl phosphonate (MeP^{2-}), and ethyl phosphonate (EtP^{2-}) (from left to right) (○). The least-squares lines are drawn through the corresponding eight data sets, which are taken for the $R-MPs$ from [25] and for the $R-PO_3$ ligands from Tables 1 and 4; the equations for these base lines are given in Table 5. The points due to the equilibrium constants for the $PMEA$ (●) and PME (⊗) systems are taken from Tables 1, 2, and 8; those for the AMP systems (⊕) are from [5]. All plotted equilibrium constant values refer to aqueous solutions at 25° and $I = 0.1M$ ($NaNO_3$).

A quantitative evaluation of the situation reflected in Fig. 2 is possible by calculating with the $pK_{H(PMEA)}^H$ value of Table 1 and the straight-line equations summarized in Table 5 the expected (calc.) stabilities for $[M(PMEA)]$ complexes having solely a phosphonate-metal-ion coordination. The corresponding results are listed in column 3 of Table 7; their

Table 7. Stability-Constant Comparisons for the $[M(\text{PMEA})]$ Complexes between the Measured Stability Constants (exper.) from Table 2 and the Calculated Stability Constants (calc.) Based on the Basicity of the Phosphonate Residue (i.e. $\text{p}K_{\text{H}(\text{PMEA})}^{\text{H}} = 6.90$; Table 1) and the Base-Line Equations Listed in Table 5 ($I = 0.1\text{M}$, NaNO_3 ; 25°C)

M^{2+}	$\log K_{[\text{M}(\text{PMEA})]}^{\text{M}}$		$\log \Delta_{\text{PMEA}}$ (Eqn. 12)
	exper.	calc.	
Mg^{2+}	1.87 ± 0.04	1.71 ± 0.03	0.16 ± 0.05
Ca^{2+}	1.65 ± 0.05	1.54 ± 0.05	0.11 ± 0.07
Sr^{2+}	1.37 ± 0.03	1.30 ± 0.04	0.07 ± 0.05
Ba^{2+}	1.30 ± 0.05	1.22 ± 0.04	0.08 ± 0.06
Mn^{2+}	2.54 ± 0.06	2.33 ± 0.05	0.21 ± 0.08
Co^{2+}	2.37 ± 0.03	2.09 ± 0.06	0.28 ± 0.07
Ni^{2+}	2.41 ± 0.05	2.11 ± 0.05	0.30 ± 0.07
Cu^{2+}	3.96 ± 0.04	3.19 ± 0.06	0.77 ± 0.07
Zn^{2+}	^{b)}	2.36 ± 0.06	$0.30 \pm 0.10^{\text{c)}$
Cd^{2+}	3.00 ± 0.04	2.67 ± 0.05	0.33 ± 0.06

a) See Footnote a of Table 2. The error limits given with the constants listed in the third column are three times the SD values given in the column farthest to the right in Table 6.

b) No stability constant could be determined due to precipitation (see also *Experimental*)^{c)}.

c) Estimated value based on the data for the Co^{2+} , Ni^{2+} , and Cd^{2+} systems; the error limit is also an estimation. These estimations furnish also an estimation for the stability of the $[\text{Zn}(\text{PMEA})]$ complex: $\log K_{[\text{Zn}(\text{PMEA})]}^{\text{Zn}} \approx 2.66 \pm 0.13$.

comparison according to Eqn. 12 with the measured (exper.) stability constants leads to the stability differences given in the fourth column of Table 7 (regarding Eqn. 12b, see Sect. 9). Evidently all the $[\text{M}(\text{PMEA})]$ complexes are more stable than expected on the basis of the basicity of the PME A-phosphonate group, though in some instances the increase is close to its error limit.

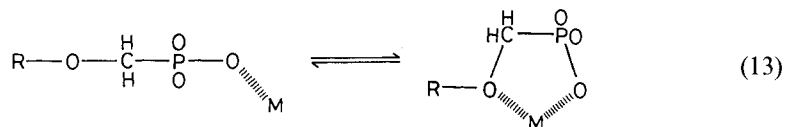
$$\log \Delta_{\text{PMEA}} = \log K_{[\text{M}(\text{PMEA})]_{\text{exper.}}}^{\text{M}} - \log K_{[\text{M}(\text{PMEA})]_{\text{calc.}}}^{\text{M}} \quad (12a)$$

$$= \log K_{[\text{M}(\text{PMEA})]_{\text{op}}}^{\text{M}} - \log K_{[\text{M}(\text{PMEA})]_{\text{op}}}^{\text{M}} \quad (12b)$$

Any kind of chelate formation must be reflected in an increased complex stability [3] [5] [35]; hence the mentioned positive stability differences prove that to some extent chelates must be formed with all these metal ions. However, exactly this fact is rather surprising, because for the alkaline earth ions and also for Mn^{2+} no or only a very weak interaction with a N donor site, e.g. N(7), is expected [5]. Indeed, comparison of the data points inserted in Fig. 2 for the $[\text{Mg}(\text{AMP})]$, $[\text{Mn}(\text{AMP})]$, and $[\text{Cu}(\text{AMP})]$ complexes [5] with those for the corresponding $[\text{M}(\text{PMEA})]$ complexes indicates that the latter ones are more stable. This observation argues against a base-back-binding of the phosphonate coordinated metal ion, e.g. to N(7), as indicated in *Equilibrium 1*.

Furthermore, the relative equality of the stability differences, $\log \Delta_{\text{PMEA}}$, given in Table 7 (except the one for Cu^{2+} ; see also Sect. 9) could be taken as a hint (cf., e.g. [35]) that an oxygen-donor site might (at least in part) be responsible for the increased stability of the $[\text{M}(\text{PMEA})]$ complexes. Indeed, inspection of the structure of the PME A^{2-} ligand (Fig. 1) reveals that an ether O-atom is located such that it could form a five-membered chelate with a phosphonate-bound metal ion. Clearly, should this actually be the cause then exactly the same stability increase should also be observable for the complexes of (phosphonylmethoxy)ethane (PME^{2-} ; cf. Fig. 1); therefore, these are addressed below.

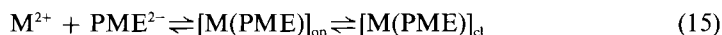
8. *Stabilities of [M(PME)] Complexes and Their Structure in Solution.* The ether O-atom is known to be able to participate in chelate formation provided it is located in a suitable position within a ligand [35]. As the R–O–CH₂–PO₃²⁻ unit of (phosphonyl-methoxy)ethane (PME²⁻) seems to fulfill this condition the following intramolecular equilibrium has to be considered (13). The position of this concentration-independent



Equilibrium 13 between an ‘open’ isomer, [M(PME)]_{op}, and a ‘closed’ species, [M(PME)]_{cl}, is defined by the intramolecular and, hence, dimension-less equilibrium constant K_1 :

$$K_1 = \frac{[[M(PME)]_{cl}]}{[[M(PME)]_{op}]} \quad (14)$$

Of course, the experimentally measured stability constant for a [M(PME)] complex is defined analogously to *Eqn. 11*, yet due to *Equilibrium 15* this expression may be rewritten as given in *Eqn. 16*, and further developed [5] [35] to *Eqns. 17* and *18*.



$$K_{[M(PME)]}^M = \frac{[[M(PME)]]}{[M^{2+}][PME^{2-}]} = \frac{([M(PME)]_{op} + [M(PME)]_{cl})}{[M^{2+}][PME^{2-}]} \quad (16)$$

$$= K_{[M(PME)]_{op}}^M + K_1 \cdot K_{[M(PME)]_{op}}^M = K_{[M(PME)]_{op}}^M \cdot (1 + K_1) \quad (17)$$

$$K_1 = \frac{K_{[M(PME)]}^M}{K_{[M(PME)]_{op}}^M} - 1 = 10^{\log A} - 1 \quad (18)$$

The stability constant of the *open* isomer, $K_{[M(PME)]_{op}}^M$, is not directly accessible by experiments, yet it may be calculated with the measurable $pK_{H(PME)}^H$ value and the equations of the correlation lines listed in *Table 5* for the ten metal ions given there. Hence, the stability-constant difference of *Eqn. 19*

$$\log A_{PME} = \log K_{[M(PME)]}^M - \log K_{[M(PME)]_{op}}^M = \log (1 + E) \quad (19)$$

(which is analogous to *Eqn. 12*) can be calculated, which then also defines the second term in the above *Eqn. 18*. It may be added that the value for $10^{\log A}$ is sometimes also addressed as the stability enhancement factor (1 + E) [35]. Clearly, knowledge of the dimension-less equilibrium constant K_1 (*Eqns. 14* and *18*) allows then to calculate, according to *Eqn. 20*, the percentage of the closed form, [M(PME)]_{cl} occurring in *Equilibrium 13*:

$$\% [M(PME)]_{cl} = 100 \cdot K_1 / (1 + K_1) \quad (20)$$

The experimental data for the M²⁺/PME systems can be completely explained by considering *Equilibria 4* and *11/15*. The corresponding stability constants (*Eqn. 16*) for the [M(PME)] complexes are listed in column 2 of *Table 8*. Comparison of these results with the calculated stability constants for the [M(PME)]_{op} species (column 3) demonstrates that the stability of *all* the [M(PME)] complexes is larger than expected on the basis of the basicity of the PME-phosphonate group (column 4); the same conclusion is

also borne out from the data points shown in *Fig. 2* for the $[M(\text{PME})]$ complexes with Mg^{2+} , Mn^{2+} , and Cu^{2+} . Evidently, *Equilibrium 13* is important for the $[M(\text{PME})]$ systems; indeed, *via Eqns. 18–20* the intramolecular equilibrium constants K_1 and the percentages for the closed species, $[M(\text{PME})]_{\text{cl}}$ can be calculated (columns 5 and 6 of *Table 8*).

Table 8. Comparison of the Measured Stability, $K_{M(\text{PME})}^M$, of the $[M(\text{PME})]$ Complexes^{a)} with the Calculated Stability $K_{[M(\text{PME})]_{\text{op}}}^M$, for an Isomer with a Sole M^{2+} /Phosphonate Coordination^{b)}, and Extent of the Intramolecular Chelate Formation (*Eqn. 13*) in the $[M(\text{PME})]$ Complexes at 25° and $I = 0.1 \text{ M}$ (NaNO_3)

M^{2+}	$\log K_{[M(\text{PME})]}^M$ (<i>Eqns. 11 and 16</i>) ^{a)}	$\log K_{[M(\text{PME})]_{\text{op}}}^M$ (<i>cf. Eqn. 15</i>) ^{b)}	$\log \Delta_{\text{PME}}$ (<i>Eqn. 19</i>) ^{c)}	K_1 (<i>Eqns. 14 and 18</i>)	% $[M(\text{PME})]_{\text{cl}}$ (<i>Eqns. 13 and 20</i>)
Mg^{2+}	1.95 ± 0.01	1.73 ± 0.03	0.22 ± 0.03	0.66 ± 0.12	40 ± 4
Ca^{2+}	1.70 ± 0.01	1.56 ± 0.05	0.14 ± 0.05	0.38 ± 0.16	28 ± 9
Sr^{2+}	1.38 ± 0.03	1.31 ± 0.04	0.07 ± 0.05	0.17 ± 0.14	15 ± 10
Ba^{2+}	1.33 ± 0.03	1.23 ± 0.04	0.10 ± 0.05	0.26 ± 0.14	21 ± 9
Mn^{2+}	2.62 ± 0.02	2.35 ± 0.05	0.27 ± 0.05	0.86 ± 0.23	46 ± 7
Co^{2+}	2.41 ± 0.02	2.12 ± 0.06	0.29 ± 0.06	0.95 ± 0.28	49 ± 7
Ni^{2+}	2.33 ± 0.02	2.14 ± 0.05	0.19 ± 0.05	0.55 ± 0.19	35 ± 8
Cu^{2+}	3.73 ± 0.03	3.25 ± 0.06	0.48 ± 0.07	2.02 ± 0.47	67 ± 5
Zn^{2+}	2.74 ± 0.02	2.40 ± 0.06	0.34 ± 0.06	1.19 ± 0.32	54 ± 7
Cd^{2+}	3.01 ± 0.02	2.71 ± 0.05	0.30 ± 0.05	1.00 ± 0.25	50 ± 6

^{a)} Determined in aqueous solution by potentiometric pH titrations; see also *Footnote a* of *Table 2*.

^{b)} Calculated with $\text{p}K_{\text{H}(\text{PME})}^{\text{H}} = 7.02$ (*Table 1*) and the reference-line equations of *Table 5*; the error limits correspond to *three times* the SD values given in the column at the right in *Table 6*.

^{c)} The errors given here and in the other two columns at the right were calculated according to the error propagation after *Gauss* by using the errors listed in the second and third column.

Clearly, this study of the M^{2+}/PME systems proves unequivocally the formation of five-membered chelates involving the $\text{R}-\text{O}-\text{CH}_2-\text{PO}_3^{2-}$ unit and supports, therefore, the suggestion made at the end of *Sect. 7* that this residue is also important for the metal-ion-coordinating properties of PMEA^{2-} .

9. *Evaluation of the Increased Stabilities of the $[M(\text{PMEA})]$ Complexes and Conclusions Regarding the Structure of These Species.* It is evident that the stability difference, $\log \Delta_{\text{PMEA}}$, for the $[M(\text{PMEA})]$ complexes as defined in *Eqn. 12b* corresponds to the definition given in *Eqn. 19* for the $[M(\text{PME})]$ complexes. Hence, the increased stabilities observed for these complexes should be compared with each other; this is best done by *Eqn. 21*

$$\Delta \log \Delta = \log \Delta_{\text{PMEA}} - \log \Delta_{\text{PME}} \quad (21)$$

The corresponding results are listed in *Table 9*: the values for $\Delta \log \Delta$ are zero within the error limits for clearly eight out of the ten cases.

This means, for the metal ions Mg^{2+} , Ca^{2+} , Sr^{2+} , Ba^{2+} , Mn^{2+} , Co^{2+} , (Zn^{2+}), and Cd^{2+} the measured increased stability of their $[M(\text{PMEA})]$ complexes can solely be explained by the formation of the five-membered chelate shown in *Equilibrium 13*, and consequently the adenine residue has no remarkable influence. Indeed, the additional calculations for K_1 and % $[M(\text{PMEA})]_{\text{cl}}$ (*Table 10*) confirm that the formation degrees for $[M(\text{PMEA})]_{\text{cl}}$

Table 9. Comparison of the Increased Stability Observed for the $[M(\text{PMEA})]$ and $[M(\text{PME})]$ Complexes in Aqueous Solution at 25° and $I = 0.1 \text{ M}$ (NaNO_3)^{a)}

M^{2+}	$\log A_{\text{PMEA}}$ (Eqn. 12) ^{b)}	$\log A_{\text{PME}}$ (Eqn. 19) ^{c)}	$\Delta \log A$ (Eqn. 21)
Mg^{2+}	0.16 ± 0.05	0.22 ± 0.03	-0.06 ± 0.06
Ca^{2+}	0.11 ± 0.07	0.14 ± 0.05	-0.03 ± 0.09
Sr^{2+}	0.07 ± 0.05	0.07 ± 0.05	0.00 ± 0.07
Ba^{2+}	0.08 ± 0.06	0.10 ± 0.05	-0.02 ± 0.08
Mn^{2+}	0.21 ± 0.08	0.27 ± 0.05	-0.06 ± 0.09
Co^{2+}	0.28 ± 0.07	0.29 ± 0.06	-0.01 ± 0.09
Ni^{2+}	0.30 ± 0.07	0.19 ± 0.05	0.11 ± 0.09
Cu^{2+}	0.77 ± 0.07	0.48 ± 0.07	0.29 ± 0.10
Zn^{2+}	$0.30 \pm 0.10^{\text{d}}$	0.34 ± 0.06	$-0.04 \pm 0.12^{\text{d}}$
Cd^{2+}	0.33 ± 0.06	0.30 ± 0.05	0.03 ± 0.08

^{a)} The error limits (3σ) are calculated according to the error propagation after Gauss.

^{b)} From Table 7.

^{c)} From Table 8.

^{d)} Estimate; see Footnote c of Table 7.

and $[\text{M}(\text{PME})]_{\text{cl}}$ are identical within the error limits for the mentioned eight metal-ion systems (cf. Tables 8 and 10), and that consequently these chelates own the same structure.

Table 10. Extent of Chelate Formation (Eqn. 13) in $[M(\text{PMEA})]$ Complexes as Quantified by the Dimensionless Equilibrium Constant K_f (analogous to Eqns. 14 and 18) and the Percentage of $[M(\text{PMEA})]_{\text{cl}}$ (analogous to Eqn. 20) in Aqueous Solution at 25° and $I = 0.1 \text{ M}$ (NaNO_3)^{a)}

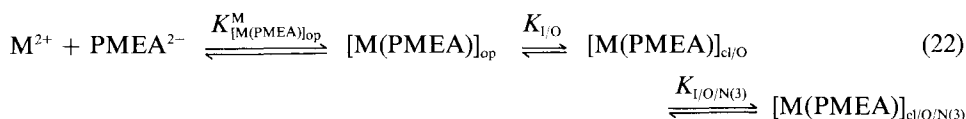
M^{2+}	$\log A_{\text{PMEA}}$ (Eqn. 12) ^{a)}	K_f (analog. Eqns. 14, 18)	% $[\text{M}(\text{PMEA})]_{\text{cl}}$ (analog. Eqn. 20)
Mg^{2+}	0.16 ± 0.05	0.45 ± 0.17	31 ± 8
Ca^{2+}	0.11 ± 0.07	0.29 ± 0.21	22 ± 13
Sr^{2+}	0.07 ± 0.05	0.17 ± 0.14	15 ± 10
Ba^{2+}	0.08 ± 0.06	0.20 ± 0.18	17 ± 12
Mn^{2+}	0.21 ± 0.08	0.62 ± 0.29	38 ± 11
Co^{2+}	0.28 ± 0.07	0.91 ± 0.29	48 ± 8
Ni^{2+}	0.30 ± 0.07	1.00 ± 0.32	50 ± 8
Cu^{2+}	0.77 ± 0.07	4.89 ± 0.98	83 ± 3
Zn^{2+}	$0.30 \pm 0.10^{\text{a)}$	1.00 ± 0.46	50 ± 12
Cd^{2+}	0.33 ± 0.06	1.14 ± 0.32	53 ± 7

^{a)} The values for $\log A_{\text{PMEA}}$ (see Eqn. 12) and their error limits (3σ) are from Table 7; see also Footnote c of Table 8. It should be noted that the results given for $[\text{Zn}(\text{PMEA})]$ are only estimates (cf. Footnote c of Table 7) and those for $[\text{Ni}(\text{PMEA})]_{\text{cl}}$ and $[\text{Cu}(\text{PMEA})]_{\text{cl}}$ are only *apparent* results, and these are, therefore, printed in *italics* as they refer to variously chelated species (see Sect. 9 and 10).

The only clear exception with a *positive* deviation of the $\Delta \log A$ values in Table 9 is the $[\text{Cu}(\text{PMEA})]$ complex. Its $\log A$ value is by *ca.* 0.3 log unit larger than the one for the $[\text{Cu}(\text{PME})]$ system. This means, the adenine residue in the $[\text{Cu}(\text{PMEA})]$ complex has a stability enhancing effect, beyond that of the ether group discussed above. Consequently, further analysis is necessary by considering additional intramolecular equilibria.

10. Intramolecular Equilibria Involving the Adenine Residue and the Ether O-Atom in $[M(\text{PMEA})]$ Complexes. The adenine moiety can only offer N(1), N(3), and N(7) for metal-ion binding (*cf.* Fig. 1). Space-filling molecular models show that a metal ion bound to the phosphonate group cannot reach N(1); this leaves N(3) and N(7) for a further coordination, and these two cases will be considered in Sect. 10.1 and 10.2, respectively.

10.1. The $[M(\text{PMEA})]$ Isomer Involving N(3). Molecular models reveal that a metal ion chelated to the phosphonate and the ether O-atom (see Eqn. 13) may also interact with N(3) by forming a seven-membered chelate without disrupting the ether O–M²⁺ bond. Therefore, the formation of a macrochelate involving only the phosphonate group and N(3) is highly unlikely; in fact, it would force the ether O-atom into the coordination sphere of the metal ion. Consequently, this leads to the successive equilibria shown in Scheme 22, where the pure phosphonate-coordinated isomer is designated as $[\text{M}(\text{PMEA})]_{\text{op}}$, the five-membered chelate involving the ether O-atom (Eqn. 13) as $[\text{M}(\text{PMEA})]_{\text{cl/O}}$ (designated in the preceding Sect. 9 as $[\text{M}(\text{PMEA})]_{\text{cl}}$) and the twofold chelated species involving also N(3) as $[\text{M}(\text{PMEA})]_{\text{cl/O/N(3)}}$.



From the Definitions 23–25

$$K_{[\text{M}(\text{PMEA})]_{\text{op}}}^{\text{M}} = \frac{[[\text{M}(\text{PMEA})]_{\text{op}}]}{[\text{M}^{2+}][\text{PMEA}^{2-}]} \quad (23)$$

$$K_{\text{I/O}} = \frac{[[\text{M}(\text{PMEA})]_{\text{cl/O}}]}{[[\text{M}(\text{PMEA})]_{\text{op}}]} \quad (24)$$

$$K_{\text{I/O/N(3)}} = \frac{[[\text{M}(\text{PMEA})]_{\text{cl/O/N(3)}}]}{[[\text{M}(\text{PMEA})]_{\text{cl/O}}]} \quad (25)$$

follows for the experimentally accessible stability constant Eqn. 26

$$K_{[\text{M}(\text{PMEA})]}^{\text{M}} = \frac{[[\text{M}(\text{PMEA})]]}{[\text{M}^{2+}][\text{PMEA}^{2-}]} = \frac{([[\text{M}(\text{PMEA})]_{\text{op}}] + [[\text{M}(\text{PMEA})]_{\text{cl/O}}] + [[\text{M}(\text{PMEA})]_{\text{cl/O/N(3)}}])}{[\text{M}^{2+}][\text{PMEA}^{2-}]} \quad (26a)$$

$$= K_{[\text{M}(\text{PMEA})]_{\text{op}}}^{\text{M}} + K_{\text{I/O}} \cdot K_{[\text{M}(\text{PMEA})]_{\text{op}}}^{\text{M}} + K_{\text{I/O}} \cdot K_{\text{I/O/N(3)}} \cdot K_{[\text{M}(\text{PMEA})]_{\text{op}}}^{\text{M}} \quad (26b)$$

$$= K_{[\text{M}(\text{PMEA})]_{\text{op}}}^{\text{M}} (1 + K_{\text{I/O}} + K_{\text{I/O}} \cdot K_{\text{I/O/N(3)}}) \quad (26c)$$

In analogy to Eqns. 14 and 18 one arrives easily [36] at the following Eqn. 27

$$K_{\text{I}} = K_{\text{I/tot}} = \frac{K_{[\text{M}(\text{PMEA})]}^{\text{M}}}{K_{[\text{M}(\text{PMEA})]_{\text{op}}}^{\text{M}}} - 1 = 10^{\log A} - 1 \quad (27a)$$

$$= \frac{[[\text{M}(\text{PMEA})]_{\text{cl/tot}}]}{[[\text{M}(\text{PMEA})]_{\text{op}}]} = \frac{([[\text{M}(\text{PMEA})]_{\text{cl/O}}] + [[\text{M}(\text{PMEA})]_{\text{cl/O/N(3)}}])}{[[\text{M}(\text{PMEA})]_{\text{op}}]} \quad (27b)$$

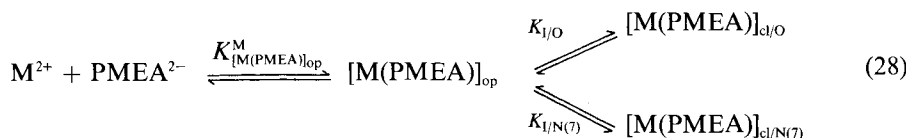
$$= K_{\text{I/O}} + K_{\text{I/O}} \cdot K_{\text{I/O/N(3)}} = K_{\text{I/O}} (1 + K_{\text{I/O/N(3)}}) \quad (27c)$$

Clearly, if the second ‘closed’ isomer, $[\text{M(PMEA)}]_{\text{cl/O/N(3)}}$, is not formed, the above equations reduce to the two-isomer problem (Eqn. 13) treated in Eqns. 14–18 with the results listed in Table 10 for the $[\text{M(PMEA)}]$ systems as discussed in Sect. 9.

The values of K_1 , which can be calculated according to Eqn. 27a, are already known (Table 10, column 3), and, therefore, also the concentrations of the open isomers, $[\text{M(PMEA)}]_{\text{op}}$. To be able to calculate the formation degree of the species that forms the five-membered chelate with the ether O-atom, i.e. $[\text{M(PMEA)}]_{\text{cl/O}}$ (Eqn. 224), the same stability is assumed for $[\text{M(PMEA)}]_{\text{cl}}$ (Sect. 8) and $[\text{M(PMEA)}]_{\text{cl/O}}$, i.e. $K_{1/\text{O}}$ for $[\text{M(PMEA)}]_{\text{cl/O}}$ equals the corresponding value for $[\text{M(PME)}]_{\text{cl}}$ (see Eqn. 13 and Fig. 1); comparison of the values of Tables 8–10 justifies this assumption. With K_1 and $K_{1/\text{O}}$ one can now calculate $K_{1/\text{O/N(3)}}$ from Eqn. 27c and hence the formation degree of the $[\text{M(PMEA)}]_{\text{cl/O/N(3)}}$ species; of course, the difference between 100 and the sum of the percentages for $[\text{M(PMEA)}]_{\text{op}}$ and $[\text{M(PMEA)}]_{\text{cl/O}}$ will also result in % $[\text{M(PMEA)}]_{\text{cl/O/N(3)}}$ and hence in $K_{1/\text{O/N(3)}}$. The results of these calculations are listed in the upper part of Table 11; they will be discussed in Sect. 10.3.

10.2. *The [M(PMEA)] Isomer Involving N(7)*. The distance to N(7) of a phosphonate-bound metal ion in a $[\text{M(PMEA)}]$ complex is rather similar to that, also to N(7), of a phosphate-bound metal-ion in a complex with AMP^{2-} (in the dominating *anti*-conformation). However, it should be emphasized that N(7) can only be reached from a phosphonate-coordinated metal ion in a $[\text{M(PMEA)}]$ complex if *no* five-membered chelate with the ether O-atom is formed. This means, the open isomer, $[\text{M(PMEA)}]_{\text{op}}$, may either transform into a macrochelate with N(7) or a five-membered chelate with the ether O-atom, but both interactions *cannot* occur at the same time in the same complex species.

These reasonings then give rise to the *Equilibrium Scheme 28*,



where $[\text{M(PMEA)}]_{\text{cl/N(7)}}$ is the macrochelated species involving N(7) and $[\text{M(PMEA)}]_{\text{cl/O}}$ is the species forming the five-membered chelate involving the ether O-atom (see Eqn. 13). The equilibrium constants $K_{[\text{M(PMEA)}]_{\text{op}}^{\text{M}}}$ and $K_{1/\text{O}}$ were defined already in Eqns. 23 and 24, respectively, and $K_{1/\text{N(7)}}$ is defined in Eqn. 29:

$$K_{1/\text{N(7)}} = \frac{[\text{M(PMEA)}]_{\text{cl/N(7)}}}{[\text{M(PMEA)}]_{\text{op}}} \quad (29)$$

Based on the *Equilibrium Scheme 28* one may derive the following equations by proceeding in the way indicated in Section 10.1:

$$K_{[\text{M(PMEA)}]_{\text{op}}^{\text{M}}} = \frac{[\text{M(PMEA)}]}{[\text{M}^{2+}][\text{PMEA}^{2-}]} = \frac{([\text{M(PMEA)}]_{\text{op}} + [\text{M(PMEA)}]_{\text{cl/O}} + [\text{M(PMEA)}]_{\text{cl/N(7)}})}{[\text{M}^{2+}][\text{PMEA}^{2-}]} \quad (30a)$$

$$= K_{[\text{M(PMEA)}]_{\text{op}}^{\text{M}}} + K_{1/\text{O}} \cdot K_{[\text{M(PMEA)}]_{\text{op}}^{\text{M}}} + K_{1/\text{N(7)}} \cdot K_{[\text{M(PMEA)}]_{\text{op}}^{\text{M}}} \quad (30b)$$

$$= K_{[\text{M(PMEA)}]_{\text{op}}^{\text{M}}} (1 + K_{1/\text{O}} + K_{1/\text{N(7)}}) \quad (30c)$$

$$K_1 = K_{1/\text{tot}} = \frac{K_{\text{M(PMEA)}}^{\text{M}}}{K_{\text{[M(PMEA)]}_{\text{op}}}^{\text{M}}} - 1 = 10^{\log d} - 1 \quad (31a)$$

$$= \frac{[[\text{M(PMEA)}]_{\text{cl}/\text{tot}}]}{[[\text{M(PMEA)}]_{\text{op}}]} = \frac{([\text{M(PMEA)}]_{\text{cl}/\text{O}}) + ([\text{M(PMEA)}]_{\text{cl}/\text{N(7)}})}{[[\text{M(PMEA)}]_{\text{op}}]} \quad (31b)$$

$$= K_{1/\text{O}} + K_{1/\text{N(7)}} \quad (31c)$$

It should be noted that the differences between *Equations 27c* and *31c* originate in the different order of the successive *Equilibria 22* and *28*. This leads to different definitions for some of the intramolecular equilibria (*Eqns. 25* and *29*), and hence to different dependencies of K_1 ($= K_{1/\text{tot}}$; see *Eqns. 27c* and *31c*), which is sometimes also addressed as the total stability enhancement *E* [35]. Of course, if the species $[\text{M(PMEA)}]_{\text{cl}/\text{N(7)}}$ is not formed then *Eqn. 31c* reduces to $K_1 = K_{1/\text{O}}$; i.e., then only *Equilibrium 13* is important.

As before in *Sect. 10.1*, the equilibrium constant $K_{1/\text{O}}$ for the $[\text{M(PMEA)}]_{\text{cl}/\text{O}}$ complexes is considered to be equal to the corresponding $[\text{M(PME)}]_{\text{cl}}$ complexes (*Eqn. 13*; *Sect. 9*); hence, $K_{1/\text{N(7)}}$ may be calculated with *Eqn. 31c*, as K_1 ($= K_{1/\text{tot}}$) is also known (*Table 10*, column 3). The results regarding the *Equilibrium Scheme 28* are listed in the lower part of *Table 11*.

10.3. *Comparison of the [M(PMEA)] Isomers Involving the Adenine Residue.* As discussed above: N(1) is not accessible for a phosphonate-bound metal ion and N(3) can only be reached, if the ether O-atom is simultaneously coordinated while with N(7) a macrochelate may be formed. The two latter possibilities involving N(3) and N(7) are displayed in the *Equilibria 22* and *28*, and the results are summarized in *Table 11*.

Table 9 and the discussion in *Sect. 9* evidence that only the $[\text{Cu(PMEA)}]$ complex owns such a significant stability increase beyond the phosphonate and ether O-atom coordination which proves unequivocally the participation of the adenine residue in complex formation. For $[\text{Ni(PMEA)}]$, such an extra stability increase is also observed, yet it is considerably smaller and just barely beyond the error limits. In any case, these two $[\text{M(PMEA)}]$ systems clearly warrant the special analysis outlined in *Sect. 10.1* and *10.2* (*cf. Table 11*). The $[\text{Cd(PMEA)}]$ system was only included into the calculations to provide the interested reader with the information how large the percentage of an extra isomer may get, without becoming significantly manifest in the experimental data.

The dimension-less 'overall' equilibrium constant K_1 ($= K_{1/\text{tot}}$; *Eqns. 27* and *31*) follows directly from the experiments (see *Sect. 9*; *Table 10*) and $K_{1/\text{O}}$ (*Eqn. 24*), which quantifies the formation of the five-membered chelate with a metal ion bound to the phosphonate group and the ether O-atom (*Eqn. 13*), has of course the same value in both equilibrium schemes (*Eqns. 22* and *28*) as it refers to the same $[\text{M(PMEA)}]_{\text{cl}/\text{O}}$ isomer; therefore, columns 3–6 and 8 contain the same results in the upper and lower parts of *Table 11*. Naturally, the values of $K_{1/\text{O}/\text{N(3)}}$ and $K_{1/\text{N(7)}}$ are different (column 7) as they refer to different intramolecular equilibria, yet the formation degrees of the $[\text{M(PMEA)}]_{\text{cl}/\text{O}/\text{N(3)}}$ (upper part) and $[\text{M(PMEA)}]_{\text{cl}/\text{N(7)}}$ isomers (lower part) are again identical (column 9). At first sight, this may seem surprising, yet the formation degree of the third isomer follows in both cases (*Eqns. 22* and *28*) from the difference, 100 minus the sum of the percentages for $[\text{M(PMEA)}]_{\text{op}}$ and $[\text{M(PMEA)}]_{\text{cl}/\text{O}}$. This means, the formation degree of the third isomer with the adenine interaction is exactly of the same size in both cases, i.e. for $[\text{M(PMEA)}]_{\text{cl}/\text{O}/\text{N(3)}}$ or $[\text{M(PMEA)}]_{\text{cl}/\text{N(7)}}$; it reaches in the $[\text{Cu(PMEA)}]$ system (rows 2, 5

Table 11. Intramolecular Equilibrium Constants (Eqns. 22 and 28) for the Formation of the Various Possible Isomeric $[M(\text{PMEA})]$ Complexes, Together with the Percentages in Which the Possible Isomers Occur in Aqueous Solution at 25° and $1 = 0.1 \text{ M } (\text{NaNO}_3)^a$

Case I Involving N(3) (Eqn. 22; Sect. 10.1)						
	$K_1 = K_{1(\text{tot})}$ (Eqn. 27a)	% $[\text{M}(\text{PMEA})]_{\text{el}(\text{tot})}$ (Eqn. 27b)	% $[\text{M}(\text{PMEA})]_{\text{op}}$ (Eqn. 27h)	$K_{1(\text{O})}$ (Eqn. 24)	$K_{1(\text{O}/\text{N}(3))}$ (Eqns. 25, 27c)	% $[\text{M}(\text{PMEA})]_{\text{el}(\text{O}/\text{N}(3))}$ (Eqn. 22 ^f)
1	Ni^{2+}	1.00 ± 0.32	50 ± 8	0.55 ± 0.19	0.82 ± 0.86	22 ± 13 (25)
2	Cu^{2+}	4.89 ± 0.98	83 ± 3	2.02 ± 0.47	1.42 ± 0.74	49 ± 10 (29)
3 ^d	Cd^{2+}	1.14 ± 0.32	53 ± 7	1.00 ± 0.25	0.14 ± 0.43	6 ± 16 (20)
Case II Involving N(7) (Eqn. 28; Sect. 10.2)						
	$K_1 = K_{1(\text{tot})}$ (Eqn. 31a)	% $[\text{M}(\text{PMEA})]_{\text{el}(\text{tot})}$ (Eqn. 31b)	% $[\text{M}(\text{PMEA})]_{\text{op}}$ (Eqn. 31b)	$K_{1(\text{O})}$ (Eqn. 24)	$K_{1(\text{O}/\text{N}(7))}$ (Eqns. 29, 31c)	% $[\text{M}(\text{PMEA})]_{\text{el}(\text{O}/\text{N}(7))}$ (Eqn. 28 ^f)
4	Ni^{2+}	1.00 ± 0.32	50 ± 8	0.55 ± 0.19	0.45 ± 0.37	22 ± 13 (19)
5	Cu^{2+}	4.89 ± 0.98	83 ± 3	2.02 ± 0.47	2.87 ± 1.09	49 ± 10 (20)
6 ^d	Cd^{2+}	1.14 ± 0.32	53 ± 7	1.00 ± 0.25	0.14 ± 0.41	6 ± 16 (19)

a) The values listed in columns 3 and 4 are from the corresponding columns in Table 10. The values given in the fifth column for % $[\text{M}(\text{PMEA})]_{\text{op}}$ follow from $100 - \% [\text{M}(\text{PMEA})]_{\text{el}(\text{tot})}$. The constants $K_{1(\text{O})}$ of column 6 are from column 5 of Table 8 (see text in Sect. 10.1); with the now known values of K_1 and $K_{1(\text{O})}$ and Eqns. 27c and 31c those for $K_{1(\text{O}/\text{N}(3))}$ and $K_{1(\text{O}/\text{N}(7))}$ may be calculated, respectively (column 7). All error limits in this table correspond to three times the standard deviation (3σ); they were calculated according to the error propagation after Gauss.

b) These results were calculated via Eqn. 24 with $K_{1(\text{O})}$ and % $[\text{M}(\text{PMEA})]_{\text{op}}$.

c) The values for % $[\text{M}(\text{PMEA})]_{\text{el}(\text{O}/\text{N}(3))}$ or % $[\text{M}(\text{PMEA})]_{\text{el}(\text{O}/\text{N}(7))}$ follow from the difference % $[\text{M}(\text{PMEA})]_{\text{el}(\text{O})} - \% [\text{M}(\text{PMEA})]_{\text{el}(\text{O}/\text{N}(3))}$ may also be calculated via Eqn. 25 with $K_{1(\text{O}/\text{N}(3))}$ and % $[\text{M}(\text{PMEA})]_{\text{el}(\text{O})}$; analogously follows % $[\text{M}(\text{PMEA})]_{\text{el}(\text{O})}$ from Eqn. 29 with $K_{1(\text{O}/\text{N}(7))}$ and % $[\text{M}(\text{PMEA})]_{\text{op}}$. The results are the same for both calculation methods (aside from small differences in the last digit due to differences in rounding) yet the error limits (which are given in parenthesis) are understandably larger for the second method.

d) The $[\text{Cd}(\text{PMEA})]$ system was included only for reasons of comparison; see text in Sect. 10.3.

in *Table 11*) *ca.* 50%, in the [Ni(PMEA)] system (rows 1, 4) *ca.* 20%, and for the [Cd(PMEA)] (rows 3, 6) and all the other systems (*cf.* *Table 10*) it is zero within the error limits what means it may occur in traces (not exceeding *ca.* 20%).

At this point the question arises: which of the adenine-bound isomers, $[M(\text{PMEA})]_{\text{cl}/\text{O}/\text{N}(3)}$ or $[M(\text{PMEA})]_{\text{cl}/\text{N}(7)}$, is acutally formed? Or, are even both isomers present at the same time? With the information presently available these questions cannot be unequivocally answered²⁾. However, careful considerations including the use of molecular models lead us to suggest that the *Equilibrium 22* involving the $[M(\text{PMEA})]_{\text{cl}/\text{O}/\text{N}(3)}$ isomer is the pertinent one. This suggestion may appear as surprising because N(3) is a very well known binding site for metal ions [3–8] [11], in contrast to N(7), yet we feel that for steric reasons N(3) is the preferred site in the $[M(\text{PMEA})]$ complexes. Indeed, the interaction of metal ions also with N(3) of a purine residue has become apparent in the past few years from X-ray crystal-structure studies of Pt^{II} complexes of guanine derivatives [38], of Rh^I complexes of 8-azaadenine derivatives [39], as well as of Ni^{II} complexes formed with neutral adenine [40], and also from solution studies with adenosine 2'-monophosphate (2'-AMP²⁻) as ligand [10]; at least Cu²⁺, possibly also Ni²⁺ and Cd²⁺ [10], forms macrochelates with 2'-AMP²⁻ involving N(3). Indeed, the formation degree of $[\text{Cu}(2'\text{-AMP})]_{\text{cl}/\text{N}(3)}$ is comparable with that of $[\text{Cu}(\text{PMEA})]_{\text{cl}/\text{O}/\text{N}(3)}$; moreover, the corresponding chelates with Ni²⁺ and Cd²⁺ form with both ligands also only in relatively low concentrations [10].

Conclusions. – 9-[2-(Phosphonylmethoxy)ethyl]adenine (PMEA) is a fascinating molecule. It resembles in many respects adenosine 5'-monophosphate (AMP²⁻; *Fig. 1*) and those properties which depend only on the qualities of the adenine moiety, like stacking interactions, H-bonding, or metal-ion coordination, as long as no sites different from those at the adenine residue are involved, are expected to be very similar or even identical. Indeed, that the adenine residue of PMEA may form adenosine-type complexes is shown by the formation of monoprotonated $[M(\text{H}\cdot\text{PMEA})]^+$ species (*Sect. 4*).

The lengths of the D-ribose 5'-monophosphate residue and of the (phosphonylmethoxy)ethane residue are also very similar; thus a metal ion coordinated at the phosphate group of AMP²⁻ or at the phosphonate group of PMEA²⁻ is placed at about the same distance from the adenine moiety, at least as long as no further interaction occurs. Of course, these equal distances could be of importance in various aspects of the biological action of both compounds and not only with regard to their metal-ion coordination.

However, there is one crucial difference between AMP²⁻ and PMEA²⁻ with regard to the structures of the metal-ion complexes formed: with AMP²⁻ alkaline earth ions only bind to the phosphate group, while divalent 3d ions and Zn²⁺ or Cd²⁺ form macrochelates involving N(7) of the adenine moiety. In contrast, with PMEA²⁻ all the metal ions studied interact not only with the phosphonate group but to a remarkable extent also with the neighboring ether O-atom, forming five-membered chelates (*Equilibrium 13*). The adenine residue of PMEA²⁻ is only exceptionally involved in metal-ion binding, as *e.g.* with Cu²⁺, and if so, most probably via N(3) (see *Sect. 10.3*).

²⁾ A study of the metal-ion systems with 9-[2-(phosphonylmethoxy)ethyl]-7-deazaadenine could answer these questions, because the replacement of N(7) by a CH unit would only allow the formation of the $[M(\text{PMEA})]_{\text{cl}/\text{O}/\text{N}(3)}$ isomer. Similar problems have been addressed before; *e.g.*, with adenosine/tubercidin [28] [37] or AMP/TuMP [5].

In other words, all enhanced complex stabilities observed so far for $[M(\text{AMP})]$ complexes could always be attributed to an interaction with N(7) [5], while the enhanced complex stability of the $[M(\text{PMEA})]$ complexes has to the largest part to be attributed to the interaction with the ether O-atom. This means, the structures of the complexes having only a phosphate or phosphonate metal-ion interaction are similar, yet those isomers, which contain chelates, are very different for AMP^{2-} and PMEA^{2-} .

Considering that the ether linkage is responsible for the mentioned different properties, it is most remarkable that exactly the same ether O-atom is important for the observation of any antiviral, *i.e.* the biological, activity of PMEA ; deletion of this O-atom or replacement by other groups leads to a loss or at least a considerable reduction of the biological activity [14] [16] [18]. Even more fascinating is that for the only other compound with comparable biological activity, *i.e.* (*S*)-9-[3-hydroxy-2-(phosphonyl-methoxy)propyl]adenine (HPMPA^{2-}) [14] [16], similar metal-ion coordinating properties are expected: metal ions coordinated to PMEA^{2-} form in equilibrium (see *Eqn. 13*) a five-membered chelate; the same is expected for HPMPA^{2-} complexes, yet, due to the structure of the residue, *i.e.* $\text{CH}_2\text{—CH}(\text{CH}_2\text{OH})\text{—O—CH}_2\text{—PO}_3^{2-}$, to an even higher formation degree, because the additional presence of the CH_2OH group allows formation of another neighboring five-membered chelate.

Considering further that the enzymes responsible for DNA synthesis (in fact practically, all enzymes which involve nucleotides as substrates) are metal-ion dependent, one wonders if the biological action of PMEA^{2-} and HPMPA^{2-} – remember, the ether O-atom is compulsory for their biological activity – does not have its origin in their metal-ion-coordinating properties. It seems quite possible that the formation of the five-membered chelates involving the ether O-atom is responsible for the inhibitory effects of PMEA and HPMPA on the growth of viruses; this chelate formation leads of course to a different orientation in space of the adenine residue than would be the case, *e.g.* with $[\text{Mg}(\text{AMP})]$ or $[\text{Zn}(\text{AMP})]$ as substrates.

The competent technical assistance of Mrs. Rita Baumbusch in the preparation of the manuscript, a research grant from the Swiss National Science Foundation (H.S.), and a fellowship to D.C. from the Amt für Ausbildungsbeiträge des Kantons Basel-Stadt are gratefully acknowledged.

REFERENCES

- [1] N. J. Leonard, *Acc. Chem. Res.* **1982**, *15*, 128.
- [2] a) G. L. Eichhorn, *Met. Ions Biol. Syst.* **1980**, *10*, 1; b) F. Y.-H. Wu, C.-W. Wu, *ibid.* **1983**, *15*, 157; c) H. R. Kalbitzer, *ibid.* **1987**, *22*, 81; d) A. S. Mildvan, *Magnesium* **1987**, *6*, 28; e) H. Sigel, A. Sigel, Eds., 'Metal Ions in Biological Systems', Vol. 25: 'Interrelations among Metal Ions, Enzymes, and Gene Expression', Marcel Dekker, New York – Basel, 1989.
- [3] H. Sigel, *Eur. J. Biochem.* **1987**, *165*, 65.
- [4] M. D. Reily, T. W. Hambly, L. G. Marzilli, *J. Am. Chem. Soc.* **1988**, *110*, 2999.
- [5] H. Sigel, S. S. Massoud, R. Tribolet, *J. Am. Chem. Soc.* **1988**, *110*, 6857.
- [6] a) R. B. Martin, Y. H. Mariam, *Met. Ions Biol. Syst.* **1979**, *8*, 57; b) R. B. Martin, *ibid.* **1988**, *23*, 315.
- [7] H. Diebler, *J. Mol. Catal.* **1984**, *23*, 209.
- [8] H. Sigel, *ACS Symp. Series* **1989**, *402*, 159.
- [9] a) R. W. Gellert, R. Bau, *Met. Ions Biol. Syst.* **1979**, *8*, 1; b) K. Aoki, 'Crystal Structures of Metal Ion-Nucleotide Complexes' in 'Landolt Börnstein, Band 1: Nukleinsäuren; Teilband b: Kristallographische und strukturelle Daten II', Ed. W. Saenger, Springer-Verlag, Berlin – Heidelberg, 1989, pp. 171; c) R. Cini, *Comments Inorg. Chem.* **1992**, *13*, 1.

- [10] S.S. Massoud, H. Sigel, *Eur. J. Biochem.* **1989**, 179, 451.
- [11] a) H. Sigel, *Coord. Chem. Rev.* **1990**, 100, 453; b) H. Sigel, *Inorg. Chim. Acta* **1992**, 198–200, 1.
- [12] J.C. Martin, Ed., 'Nucleotide Analogues as Antiviral Agents', ACS Symposium Series 401; American Chemical Society, Washington, DC, 1989.
- [13] R. Tribolet, H. Sigel, *Eur. J. Biochem.* **1987**, 163, 353.
- [14] A. Holý, E. De Clercq, I. Votruba, *ACS Symp. Series* **1989**, 401, 51.
- [15] E. De Clercq, A. Holý, I. Rosenberg, *Antimicrob. Agents Chemother.* **1989**, 33, 185.
- [16] A. Holý, I. Votruba, A. Merta, J. Černý, J. Veselý, J. Vlach, K. Šedivá, I. Rosenberg, M. Otmar, H. Hřebabecký, M. Trávníček, V. Vonka, R. Snoeck, E. De Clercq, *Antiviral Res.* **1990**, 13, 295.
- [17] R. Pauwels, J. Balzarini, D. Schols, M. Baba, J. Desmyter, I. Rosenberg, A. Holý, E. De Clercq, *Antimicrob. Agents Chemother.* **1988**, 32, 1025.
- [18] A. Holý, *Il Farmaco* **1991**, 46 (Suppl. 1), 141.
- [19] a) A. Holý, I. Rosenberg, *Collect. Czech. Chem. Commun.* **1987**, 52, 2801; b) A. Holý, I. Rosenberg, H. Dvořáková, *ibid.* **1989**, 54, 2190.
- [20] F. Gregáň, V. Kettmann, P. Novomeský, submitted to *Synthesis*.
- [21] H. Sigel, A. D. Zuberbühler, O. Yamauchi, *Anal. Chim. Acta* **1991**, 255, 63.
- [22] M. Bastian, H. Sigel, *J. Coord. Chem.* **1991**, 23, 137.
- [23] a) H. Sigel, *Biol. Trace Elem. Res.* **1989**, 21, 49; b) K. H. Scheller, F. Hofstetter, P. R. Mitchell, B. Prijs, H. Sigel, *J. Am. Chem. Soc.* **1981**, 103, 247.
- [24] R. Tribolet, H. Sigel, *Biophys. Chem.* **1987**, 27, 119.
- [25] S.S. Massoud, H. Sigel, *Inorg. Chem.* **1988**, 27, 1447.
- [26] a) N. Wiberg, (Holleman-Wiberg), 'Lehrbuch der Anorganischen Chemie' (91th–100th edn.), Walter de Gruyter-Verlag, Berlin – New York, 1985, p. 651; b) R. C. Weast, M. J. Astle, Eds., 'CRC Handbook of Chemistry and Physics', CRC Press, Boca Raton, Florida, 1982, p. D-173; c) 'Gmelins Handbuch der Anorganischen Chemie', 8th edn., 'Phosphor', Teil C, System-Nr. 16, Verlag Chemie GmbH, Weinheim, 1965, p. 127.
- [27] H. Brintzinger, G. G. Hammes, *Inorg. Chem.* **1966**, 5, 1286.
- [28] H. Sigel, N. A. Corfù, L.-n. Ji, R. B. Martin, *Comments Inorg. Chem.* **1992**, 13, 35.
- [29] G. Liang, N. A. Corfù, H. Sigel, *Z. Naturforsch., B* **1989**, 44, 538.
- [30] H. Sigel, K. Becker, D. B. McCormick, *Biochim. Biophys. Acta* **1967**, 148, 655.
- [31] H. Irving, R. J. P. Williams, *Nature (London)* **1948**, 162, 746; *J. Chem. Soc.* **1953**, 3192.
- [32] H. Sigel, D. B. McCormick, *Acc. Chem. Res.* **1970**, 3, 201.
- [33] H. Sigel, R. Tribolet, R. Malini-Balakrishnan, R. B. Martin, *Inorg. Chem.* **1987**, 26, 2149.
- [34] H. Brintzinger, *Helv. Chim. Acta* **1965**, 48, 47.
- [35] R. B. Martin, H. Sigel, *Comments Inorg. Chem.* **1988**, 6, 285.
- [36] H. Sigel, *Coord. Chem. Rev.* **1993**, 122, 227.
- [37] L.-n. Ji, N. A. Corfù, H. Sigel, *J. Chem. Soc., Dalton Trans.* **1991**, 1367.
- [38] G. Raudaschl-Sieber, H. Schöllhorn, U. Thewalt, B. Lippert, *J. Am. Chem. Soc.* **1985**, 107, 3591.
- [39] W. S. Sheldrick, B. Günther, *Inorg. Chim. Acta* **1988**, 152, 223.
- [40] a) A. Ciccarese, D. A. Clemente, A. Marzotto, M. Rosa, G. Valle, *J. Inorg. Biochem.* **1991**, 43, 470; b) A. Marzotto, G. Valle, D. A. Clemente, 'Abstracts of the 29th Internat. Conf. on Coordination-Chem.' (Lausanne, Switzerland, July 19–24), 1992, p. 72, No. P182.